STATISTICS, OPTIMIZATION AND INFORMATION COMPUTING
Stat., Optim. Inf. Comput., Vol. **15**, April 2026, pp 3282–3304.
Published online in International Academic Press (www.IAPress.org)

Optimal Control Problem of Mathematical Model with Fuzzy Parameter for the COVID-19 Epidemic with Symptomatic and Asymptomatic cases in Indonesia

Muhammad Kharis [1], Miswanto [2,*], Cicik Alfiniyah [2]

[1] *Doctoral Program of Mathematics and Sciences, Faculty of Science and Technology, Universitas Airlangga, Surabaya 60115, Indonesia*
[2] *Department of Mathematics, Faculty of Science and Technology, Universitas Airlangga, Surabaya 60115, Indonesia*

Abstract In this study, we analyze the optimal control model for the COVID-19 epidemic in Indonesia, considering both symptomatic and asymptomatic cases, and considering government policies. We used three control parameters: policies to prevent the spread of the disease among vulnerable people, quarantine with treatment for symptomatic patients, and infection testing followed by isolation for asymptomatic patients. To obtain the optimal solution, the Pontryagin Maximum Principle and cost-effectiveness analysis methods were used. Based on the cost-effectiveness analysis, it was concluded that implementing the three control measures simultaneously at each temperature was significantly more cost-effective in preventing the spread of infection than when only one or two controls were implemented. Another interesting finding was the emergence of symptomatic patients again if preventive controls were reduced, while asymptomatic patients still existed.

Keywords COVID-19, symptomatic and asymptomatic cases, optimal control, objective function, cost-effectiveness analysis

AMS 2010 subject classifications 49J15, 49M05, 92D30

DOI: 10.19139/soic-2310-5070-3123

1. Introduction

The COVID-19 outbreak was first detected in late December 2019 in Wuhan City, Hubei Province, China, as a cluster of pneumonia cases with a novel cause later identified as the SARS-CoV-2 virus [1]. Genetic sequencing and initial clinical reports suggested human-to-human transmission and an epidemiological link to a Wuhan animal market [2, 3]. Since these initial reports, cases have spread rapidly through international travel and community transmission, leading the World Health Organization (WHO) to declare a Public Health Emergency (PHEIC) on January 30, 2020, and a pandemic on March 11, 2020 [4].

In Indonesia, the first case was announced on March 2, 2020, and within weeks, it had spread to many provinces. Epidemiological characteristics include a significant proportion of asymptomatic or pre-symptomatic infections, complicating early detection and facilitating hidden transmission. International meta-analyses and local studies indicate that the proportion of asymptomatic infections is significant, necessitating a massive testing and tracing strategy [5, 6]. Without proactive policies to detect asymptomatic infections, such as rapid contact tracing, prolonged pandemic control efforts may be necessary, even with vaccination [6]. The high percentage of asymptomatic infections highlights the potential risk of asymptomatic transmission in the community [5]. Effective supportive therapy and strict social distancing are crucial in preventing the spread of the disease from asymptomatic

*Correspondence to: Miswanto (Email: miswanto@fst.unair.ac.id). Department of Mathematics, Faculty of Science and Technology, Universitas Airlangga, Surabaya 60115, Indonesia.

ISSN 2310-5070 (online) ISSN 2311-004X (print)

Table 1. The definition of the parameter in the model

Parameter	Definition
B	the rate of immigration
p_1	the proportion of quarantined persons free from infection
p_2	the vaccination rate of susceptible persons
p_3	the percentage of symptomatic infected persons
p_4	the rate of infected persons who get quarantine and treatments
ω	the birth rate
μ	the natural death rate
α	the rate of persons out of quarantine
β	the probability of susceptible persons becoming infected after contacting infected persons
η	the effectiveness of vaccination
m_1, m_2	the death rate due to infection
γ	the recovery rate

or mildly symptomatic individuals [7]. The Indonesian government responded with large-scale social restrictions (PSBB), leveled PPKM restrictions, a testing-tracing-isolation program, and a mass vaccination program since 2021—these policies have been reviewed in the literature assessing the effectiveness of mobility controls and public interventions in curbing transmission [8, 9].

Sasmita *et al.* [10] examined optimal control in a mathematical model of the COVID-19 outbreak in Indonesia. In their model, control measures include large-scale social restrictions (u_1), contact tracing (u_2), mass rapid antibody testing (u_3), case detection and treatment (u_4), and the wearing of face masks (u_5). The analyzed model takes the form of $SEI2RS$, where E, I_1, and I_2 represent the exposed, carrier, and infectious classes, respectively. The exposed class represents individuals suspected of being infected, the carrier class represents undetected individuals, and the infectious class represents detected individuals. Furthermore, the research on the mathematical model of optimal control in the COVID-19 outbreak that underlies this study is the research conducted in [11], which examines the optimal control of COVID-19 in Indonesia with fuzzy parameters using temperature as a crisp variable. The model in [11] is the QSIQR mathematical model, which still does not include cases of asymptomatic infection, and also the control used still uses two controls: preventive control against the possibility of disease transmission in susceptible individuals and quarantine for infected individuals. In this study, optimal control will be studied by improving the QSIQR model, namely by adding a class of infected individuals without symptoms and also adding one control: infection testing followed by quarantine for infected individuals without symptoms. The definition of fuzzy parameters uses the definition in [11], whose basic idea is obtained from [12]. The fuzzy membership functions in [12] have been formulated for several parameters in the SIR model, where the size of the virus in the body is a crisp variable. In this study, the temperature is used as a crisp variable and the present study focuses on the early-to-mid pandemic period.

2. Materials And Methods

2.1. Model Formulation

We defined the Quarantined-Susceptible-Symptomatic and Asymptomatic Infected-Quarantined-Recovered $(QSIAQR)$ model. The model assumes a homogeneous population, which is a common simplification in optimal control epidemic modelling aimed at evaluating population-level intervention strategies rather than individual risk stratification. The definition of each variable, namely S, I, A, and R, respectively, represents the number of susceptible individuals, infected with symptoms, infected without symptoms, and recovered. The variable Q_1 indicates the number of individuals quarantined from immigration, while Q_T states the number of infected individuals undergoing quarantine. The transfer diagram is shown in Fig. 1, while the explanation for each parameter is presented in Table 1.

Kementerian Kesehatan Republik Indonesia/The Indonesian Ministry of Health [13] reported that most deaths due to Covid-19 in Indonesia occurred in patients with comorbidities, such as heart disease, diabetes, and

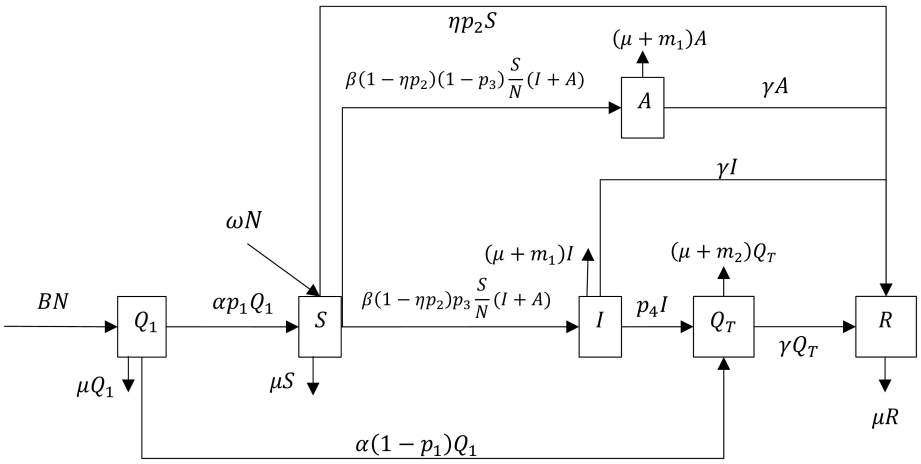

Figure 1. The transfer diagram of the QSIAQR model

respiratory disorders. Conversely, patients undergoing centralized isolation or quarantine with mild to moderate symptoms had a very high recovery rate. Furthermore, according to Kompas [14], the mortality rate for fully vaccinated Covid-19 patients—most of whom were in the centralized quarantine group—was only 0.21%. Research by Bi et al. [15] also indicated that the severity of symptoms and mortality rates were very low, especially among individuals identified and quarantined early. No deaths were found among quarantined close contacts, further strengthening the evidence of quarantine's effectiveness in suppressing infection severity. Based on these findings, it can be concluded that the mortality rate in the subpopulation quarantined due to infection is very small, so it can be assumed to be close to zero in mathematical modeling. Every arrival from immigration is required to undergo quarantine based on government policy requiring all arrivals from countries or regions affected by infectious diseases to undergo health quarantine. This policy is stated in regulations issued by Pemerintah Pusat Indonesia/ the Indonesian Central Government [16, 17] and Satuan Tugas Penanganan COVID-19/ the COVID-19 Handling Task Force [18].

In this research, we assumed that the birth rate has the same value as the natural death rate. Hence, $\omega = \mu$, and $m_2 = 0$, then based on Fig. 1, we got System (1).

$$\begin{array}{lcl}
\frac{dQ_1}{dt} & = & BN - (\alpha+\mu)Q_1 \\
\frac{dS}{dt} & = & \mu N + \alpha p_1 Q_1 - \beta(1-\eta p_2)\frac{S(I+A)}{N} - (\eta p_2 + \mu)S \\
\frac{dI}{dT} & = & \beta(1-\eta p_2)p_3\frac{S(I+A)}{N} - (p_4+\gamma+\mu+m_1)I \\
\frac{dA}{dt} & = & \beta(1-\eta p_2)(1-p_3)\frac{S(I+A)}{N} - (\gamma+\mu+m_1)A \\
\frac{dQ_T}{dt} & = & \alpha(1-p_1)Q_1 + p_4 I - (\gamma+\mu)Q_T \\
\frac{dR}{dt} & = & \eta p_2 S + \gamma(I+A+Q_T) - \mu R \\
N & = & Q_1 + S + I + A + Q_T + R
\end{array} \tag{1}$$

We give the initial condition of every variable in the System (1) such that

$$Q_1(0) \geq 0, S(0) \geq 0, I(0) > 0, A \geq 0, Q_T(0) \geq 0, R(0) \geq 0 \tag{2}$$

2.2. Parameter Estimation and Data Fitting

This subsection conducts parameter estimation and model validation using data from various sources. Indonesian population data based on the 2020 Census was obtained from Badan Pusat Statistik (the Central Statistics Agency)

Table 2. The definition of the parameter in the model

Parameter	value	Parameter	value
B	0.000238670	β	0.914678487
μ	0.0000357	p_1	0.993317838
α	0.142857143	p_2	0.0042960296
m_1	0.001946408	p_3	0.980632535
η	0.95	p_4	0.970732435
γ	0.063065477		

[19], with a total population of 270,203,917. The parameter $\mu = 0.0000357$ was taken from [20], assuming a life expectancy of approximately 77 years for the Indonesian population. COVID-19 epidemic data was sourced from [21], which includes the number of new deaths and recoveries from July 12, 2021, to November 30, 2021. From these data, the parameters $m_1 = 0.001946408$ and $\gamma = 0.063065477$ were obtained. The quarantine period for arrivals ranges from 7 to 14 days, so the estimated α value is in the range of 0.07142 to 0.14286. Meanwhile, Nasir et al. in [22] reported that vaccine effectiveness (η) was in the range of 62.1%–95%.

The parameters B, β, p_1, p_2, p_3, and p_4 were estimated using the fourth-order Runge–Kutta method. This estimation was based on 142 data points on the number of infected cases from July 12, 2021, to November 30, 2021. This period was chosen because it represented the peak of the COVID-19 outbreak. The estimation results provide a value of $B = 0.000238670, \beta = 0.914678487, p_1 = 0.993317838, p_2 = 0.0042960296, p_3 = 0.980632535$, and $p_4 = 0.970732435$, with a Mean Absolute Percentage Error (MAPE) of 0.210008, which indicates a good enough model accuracy. The initial values of the variables are set as $Q_{10} = 139433, I_0 = 376015$, and $R_0 = 2084724$, assuming $Q_{T0} = I_0, A_0 = \frac{I_0}{3}$ and $S_0 = N_0 - (Q_{10} + I_0 + A_0 + Q_{T0} + R_0)$, where $N_0 = 270203917$. The comparison between the actual data $I(t)$ and the estimated results of the $I(t)$ model is shown in Fig. 2, while the complete list of parameter values is presented in Table 2.

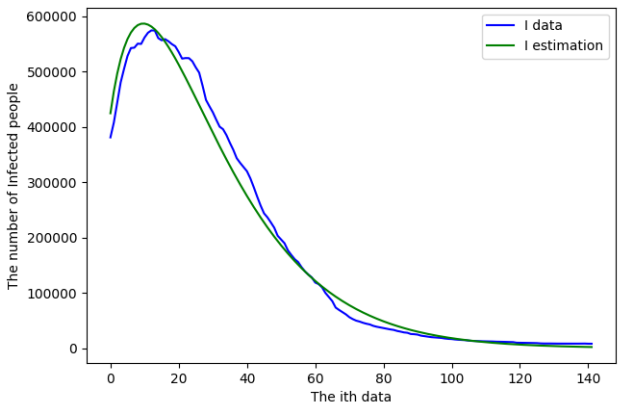

Figure 2. Graphic of I data and I estimation

2.3. Global sensitivity analysis of epidemic parameter

In this section, sensitivity analysis using Latin Hypercube Sampling and Partial Rank Correlation Coefficient (LHS/PRCC) on parameters $B, \beta, p_1, p_2, p_3, p_4$ was carried out with the number of samples = 2000. The results of this analysis are given in Table 3.

The results of the global sensitivity analysis in Table 3 have shown that parameter p_3 is the most dominant parameter in influencing system dynamics, with a very strong negative correlation with model output. The parameter β is in second place with a strong positive influence. All parameters show high statistical significance

Table 3. The sensitivity index of parameters in model

Parameter	Baseline	Range	Distribution	PRCC	95% CI	p-value	Rank
p_3	0.98063253	(0.78451, 1.0)	uniform	-0.712	[-0.733, -0.689]	< 0.001	1
β	0.91467849	(0.73174, 1.0)	uniform	0.537	[0.505, 0.567]	< 0.001	2
p_1	0.99331784	(0.79465, 1.0)	uniform	0.423	[0.386, 0.458]	< 0.001	3
B	0.00023867	(0.00019094, 0.00028640)	uniform	0.417	[0.380, 0.453]	< 0.001	4
p_2	0.00429603	(0.00344, 0.00516)	uniform	0.350	[0.311, 0.388]	< 0.001	5
p_4	0.97073244	(0.77659, 1.0)	uniform	0.264	[0.222, 0.304]	< 0.001	6

($p < 0.001$), indicating that variations in these parameters significantly influence epidemic dynamics. p_3 has a very strong negative correlation with the model output, meaning that if p_3 increases, the number of infected people decreases, and vice versa, if p_3 decreases, the number of infected people increases. Logically, if the percentage of infected people with symptoms (can be detected) increases, outbreak control is easier to implement. Conversely, if the percentage of infected people without symptoms (not yet detected) increases, outbreak control is more difficult, causing the probability of infection transmission to increase.

2.4. The membership function of the fuzzy parameter

In this study, environmental influences are limited to temperature only where humidity is assumed to be constant. This is done to maintain model simplicity and interpretability. Additional environmental variables are recognized as important extensions but are beyond the scope of the current analysis. The membership function of fuzzy parameters β and p_4 are obtained from [11].

$$\beta(T) = \begin{cases} \beta_{min} & T < T_{min}, \\ \beta_{min} + \beta_1(1-\pi)(1-\theta)\frac{T-T_{min}}{T_{opt}-T_{min}} & T_{min} \le T \le T_{opt}, \\ \beta_{min} + \beta_1(1-\pi)(1-\theta)\frac{T_{max}-T}{T_{max}-T_{opt}} & T_{opt} \le T < T_{max}, \\ \beta_{min} & T \ge T_{max}. \end{cases} \tag{3}$$

where $\beta_{min} = 1 - \beta_1(1-\pi)(1-\theta)$

$$p_4(T) = \begin{cases} 1 - c.Y_{(\pi,\theta)} & T < T_{min}, \\ 1 - c.Y_{(\pi,\theta)}[1 - \frac{T-T_{min}}{T_{opt}-T_{min}}] & T_{min} \le T \le T_{opt}, \\ 1 - c.Y_{(\pi,\theta)}[1 - \frac{T_{max}-T}{T_{max}-T_{opt}}] & T_{opt} \le T < T_{max}, \\ 1 - c.Y_{(\pi,\theta)} & T \ge T_{max}. \end{cases} \tag{4}$$

where $Y_{(\pi,\theta)} = [\beta_{min} + \beta_1(1-\pi)(1-\theta)]$

Parameter β_1 is the standard virus transmission probability based on the characteristics of the virus, π is the proportion of susceptible persons who are implementing health protocols, θ is the effectiveness of government policies like vaccination and quarantine, and c is the weight of β for p_4. T_{min}, T_{opt}, and T_{max} successively are minimum, optimum, and maximum temperatures ($^\circ C$). The spread of COVID-19 has a range of optimal temperatures from $13^\circ C$ to $24^\circ C$, where cities with temperatures below $24^\circ C$ are categorized as high-risk areas for transmission [23]. The temperature range that does not have a significant impact on the spread of COVID-19 is between $26^\circ C$–$30^\circ C$ with humidity above 60% [24]. Kerobe *et al.* [25] confirmed a negative correlation between temperature and humidity parameters and the rate of virus transmission. This finding implies that the risk of disease transmission in the community tends to decrease significantly when environmental conditions become warmer or more humid. Ng *et al.* [26] showed that increases in maximum temperature, average temperature, minimum temperature, and average relative humidity were all inversely related to the number of confirmed COVID-19 cases. Liu *et al.* [27] found that in low-temperature environments, increasing temperatures were only followed by an increase in the number of new daily cases (a positive relationship). Conversely, the suppressive effect of new viruses was consistently seen (a negative relationship) when air temperatures were already at higher levels. This

Table 4. The value of β and p_4 based on T (Source: [11])

T	β	p_4	$\frac{p_4}{\beta}$
$7^\circ C$	0.960136	0.866667	0.90265
$10^\circ C$	0.980068	0.933333	0.95231
$22.5^\circ C$	1	1	1
$25^\circ C$	0.970102	0.9	0,92774

suggests that the effectiveness of temperature in suppressing a pandemic is highly dependent on the temperature threshold in the region.

From [11], we get $\beta_1 = 0.99, T_{min} = 4, 13 \leq T_{opt} \leq 24, T_{max} = 26, \pi = 0.8, \theta = 0.698$ and $c = 0.2$. The value of β and p_4 based on T are given in Table 4.

The graphs of I and A without control are given in Fig. 3.

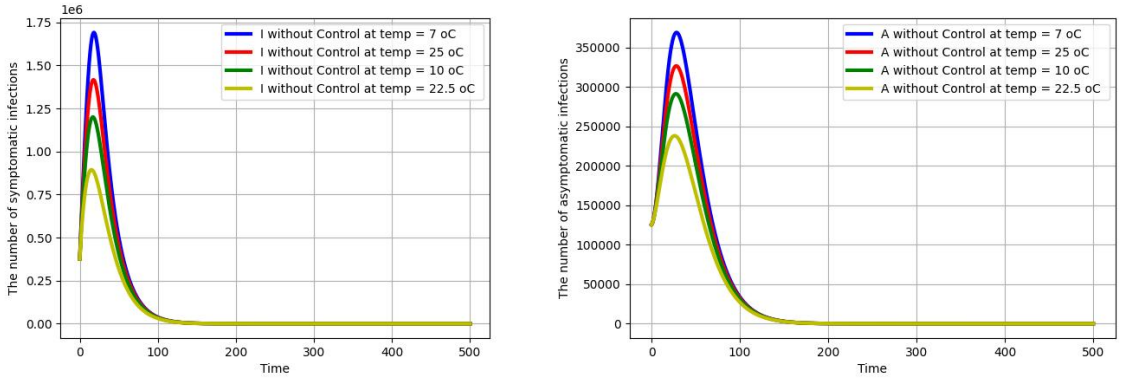

Figure 3. The graphs of I and A without control

From Table 4 and Fig. 3, the epidemic will disappear more quickly if the ratio of the quarantine rate of infected people and the rate of infection is greater.

2.5. Control Optimal Model

We added three control parameters to System (1), and let $\beta(T) = \hat{\beta}, p_4(T) = \hat{p_4}$ then we got System (5).

$$\begin{array}{lcl}
\frac{dQ_1}{dt} & = & BN - (\alpha + \mu)Q_1 \\
\frac{dS}{dt} & = & \mu N + \alpha p_1 Q_1 - (1-u_1)\hat{\beta}(1-\eta p_2)\frac{S(I+A)}{N} - (\eta p_2 + \mu)S \\
\frac{dI}{dT} & = & (1-u_1)\hat{\beta}(1-\eta p_2)p_3\frac{S(I+A)}{N} - (\hat{p_4} + u_2 + \gamma + \mu + m_1)I \\
\frac{dA}{dt} & = & (1-u_1)\hat{\beta}(1-\eta p_2)(1-p_3)\frac{S(I+A)}{N} - (\gamma + \mu + m_1 + u_3)A \\
\frac{dQ_T}{dt} & = & \alpha(1-p_1)Q_1 + (\hat{p_4} + u_2)I + u_3 A - (\gamma + \mu)Q_T \\
\frac{dR}{dt} & = & \eta p_2 S + \gamma(I + A + Q_T) - \mu R \\
N & = & Q_1 + S + I + A + Q_T + R
\end{array} \tag{5}$$

The meaning of the control parameters are

u_1 : policies to prevent the spread of disease among susceptible people
i.e. wearing masks, maintaining distance/physical contact, and vaccination

u_2 : quarantine and treatment efforts for infected persons with symptoms

u_3 : infection testing followed by quarantine for infected persons without symptoms

In this study, the control variables u_1, u_2, and u_3 are formulated as continuous intervention intensities endogenously determined by the optimal control framework, rather than as rule-based policy triggers.

Consequently, the model captures gradual adjustments in control intensity driven by epidemiological dynamics, instead of relying on predefined threshold-based exit criteria. While explicit policy milestones may be useful for operational decision-making, their specification lies beyond the normative scope of the present analysis and is left for future applied studies.

Let $U = \{(u_1(t), u_2(t), u_3(t)) : 0 \leq u_1 \leq 1, 0 \leq u_2 \leq 1, 0 \leq u_3 \leq 1, 0 < t < t_f\}$ is the set of receivable controls. The goal is to find a control u or a combination of some controls u that produces the lowest value for the objective function J without sacrificing the cost efficiency of implementation in System (5).

Let

$$J = \min_{(u_1,u_2,u_3)} \int_0^{t_f} \left(I + A + \frac{1}{2} \sum_{i=1}^{3} w_i u_i^2 \right) dx \tag{6}$$

Subject to (5), where w_1, w_2, and w_3 are positive constants representing the relative cost weights for implementing control efforts u_1, u_2, and u_3. We assumed that the costs were non-linear. Hence, the control variables in the objective function J are in the form of second-degree polynomials [29, 28]. The second-degree (quadratic) polynomial is deliberately chosen as a standard assumption in optimal control theory to ensure convexity, analytical tractability, and the existence of interior optimal solutions. Our main objective is to minimize the number of people exposed and affected by the disease while keeping the control costs as low as possible. Thus, we are going to find optimal controls (u_1^*, u_2^*, u_3^*), such that

$$J(u_1^*, u_2^*, u_3^*) = \min \{J(u_1, u_2, u_3) : (u_1, u_2, u_3) \in U\} \tag{7}$$

where u_1, u_2, and u_3 are measurable with $0 \leq u_i \leq 1, i = 1, 2, 3$ for $t \in [0, t_f]$.

3. Results

3.1. The Hamiltonian and optimality system

The optimal solution is obtained by formulating the necessary conditions for applying the Pontryagin Maximum Principle [30]. Therefore, this principle converts the Equations (5) and (6) into a problem of minimizing a Hamiltonian, H, pointwise concerning u_1, u_2, and u_3, and a Hamiltonian (H) can be defined as:

$$H(t, x(t), u(t), \lambda(t)) = f(t, x(t), u(t)) + \lambda g(t, x(t), u(t)) \tag{8}$$

where

$$\begin{aligned}
f(t, x(t), u(t)) &= I + A + \tfrac{1}{2} w_1 u_1^2 + \tfrac{1}{2} w_2 u_2^2 + \tfrac{1}{2} w_3 u_3^2, \\
g(t, x(t), u(t)) &= (g_1, g_2, g_3, g_4, g_5, g_6)^T, \\
g_1 &= BN - (\alpha + \mu) Q_1 \\
g_2 &= \mu N + \alpha p_1 Q_1 - (1 - u_1)\hat{\beta}(1 - \eta p_2)\tfrac{S(I+A)}{N} - (\eta p_2 + \mu) S \\
g_3 &= (1 - u_1)\hat{\beta}(1 - \eta p_2) p_3 \tfrac{S(I+A)}{N} - (\hat{p_4} + u_2 + \gamma + \mu + m_1) I \\
g_4 &= (1 - u_1)\hat{\beta}(1 - \eta p_2)(1 - p_3)\tfrac{S(I+A)}{N} - (\gamma + \mu + m_1 + u_3) A \\
g_5 &= \alpha(1 - p_1) Q_1 + (\hat{p_4} + u_2) I + u_3 A - (\gamma + \mu) Q_T \\
g_6 &= \eta p_2 S + \gamma(I + A + Q_T) - \mu R \\
N &= Q_1 + S + I + A + Q_T + R,
\end{aligned}$$

$Q_1(0) \geq 0, S(0) \geq 0, I(0) > 0, A > 0, Q_T(0) \geq 0$, and $R(0) \geq 0$.

Hence, the Hamiltonian becomes

$H(t, Q_1, S, I, A, Q_T, R)$

$= f(t, I, A, u_1, u_2, u_3) + \lambda_1 \frac{dQ_1}{dt} + \lambda_2 \frac{dS}{dt} + \lambda_3 \frac{dI}{dt} + \lambda_4 \frac{dA}{dt} + \lambda_5 \frac{dQ_T}{dt} + \lambda_6 \frac{dR}{dt}$

Hence,

$H = I + A + \frac{1}{2}w_1u_1^2 + \frac{1}{2}w_2u_2^2 + \frac{1}{2}w_3u_3^2 + \lambda_1 g_1 + \lambda_2 g_2 + \lambda_3 g_3 + \lambda_4 g_4 + \lambda_5 g_5 + \lambda_6 g_6$
where $\lambda_i, i = 1, 2, ..., 6$ are adjoint variables with transversality conditions $\lambda_i(t_f) = 0, i = 1, 2, ..., 6$ for an optimal control (u_1^*, u_2^*, u_3^*) that minimizes $J(u_1, u_2, u_3)$ and $\frac{d\lambda}{dt} = -\frac{\partial H}{\partial X}$ where $X = (Q_1, S, I, A, Q_T, R)^T$ and $\lambda = (\lambda_1, \lambda_2, \lambda_3, \lambda_4, \lambda_5, \lambda_6)^T, \lambda(t_f) = 0$ transcendentality condition.

Hence,

$$\begin{aligned}
\tfrac{d\lambda_1}{dt} &= -\tfrac{\partial H}{\partial Q_1} \\
&= -\lambda_1(B-\alpha-\mu) - \lambda_2\left((1-u_1)\hat{\beta}(1-\eta p_2)\tfrac{S(I+A)}{N^2} + \alpha p_1 + \mu\right) \\
&\quad +\lambda_3(1-u_1)\hat{\beta}(1-\eta p_2)p_3\tfrac{S(I+A)}{N^2} + \lambda_4(1-u_1)\hat{\beta}(1-\eta p_2)(1-p_3)\tfrac{S(I+A)}{N^2} - \lambda_5\alpha(1-p_1) \\
\tfrac{d\lambda_2}{dt} &= -\tfrac{\partial H}{\partial S} \\
&= -\lambda_1 B - \lambda_2\left((1-u_1)\hat{\beta}(1-\eta p_2)\tfrac{S(I+A)}{N^2} - (1-u_1)\hat{\beta}(1-\eta p_2)\tfrac{(I+A)}{N} - \eta p_2\right) \\
&\quad -\lambda_3\left((1-u_1)\hat{\beta}(1-\eta p_2)p_3\tfrac{(I+A)}{N} - (1-u_1)\hat{\beta}(1-\eta p_2)p_3\tfrac{S(I+A)}{N^2}\right) \\
&\quad -\lambda_4\left((1-u_1)\hat{\beta}(1-\eta p_2)(1-p_3)\tfrac{(I+A)}{N} - (1-u_1)\hat{\beta}(1-\eta p_2)(1-p_3)\tfrac{S(I+A)}{N^2}\right) - \lambda_6\eta p_2 \\
\tfrac{d\lambda_3}{dt} &= -\tfrac{\partial H}{\partial I} \\
&= -\lambda_1 B - \lambda_2\left((1-u_1)\hat{\beta}(1-\eta p_2)\tfrac{S(I+A)}{N^2} - (1-u_1)\hat{\beta}(1-\eta p_2)\tfrac{S}{N} + \mu\right) \\
&\quad -\lambda_3\left((1-u_1)\hat{\beta}(1-\eta p_2)p_3\tfrac{S}{N} - (1-u_1)\hat{\beta}(1-\eta p_2)p_3\tfrac{S(I+A)}{N^2} - \gamma - m_1 - \mu - \hat{p_4} - u_2\right) \\
&\quad -\lambda_4\left((1-u_1)\hat{\beta}(1-\eta p_2)\tfrac{S}{N} - (1-u_1)\hat{\beta}(1-\eta p_2)(1-p_3)\tfrac{S(I+A)}{N^2}\right) - \lambda_5(\hat{p_4} + u_2) - \lambda_6\gamma - 1 \\
\tfrac{d\lambda_4}{dt} &= -\tfrac{\partial H}{\partial A} \\
&= -\lambda_1 B - \lambda_2\left((1-u_1)\hat{\beta}(1-\eta p_2)\tfrac{S(I+A)}{N^2} - (1-u_1)\hat{\beta}(1-\eta p_2)\tfrac{S}{N} + \mu\right) \\
&\quad -\lambda_3\left((1-u_1)\hat{\beta}(1-\eta p_2)p_3\tfrac{S}{N} - (1-u_1)\hat{\beta}(1-\eta p_2)p_3\tfrac{S(I+A)}{N^2}\right) \\
&\quad -\lambda_4\left((1-u_1)\hat{\beta}(1-\eta p_2)(1-p_3)\tfrac{S}{N} - (1-u_1)\hat{\beta}(1-\eta p_2)(1-p_3)\tfrac{S(I+A)}{N^2} - \gamma - m_1 - \mu - u_3\right) \\
&\quad -\lambda_5 u_3 - \lambda_6\gamma - 1 \\
\tfrac{d\lambda_5}{dt} &= -\tfrac{\partial H}{\partial Q_T} \\
&= -\lambda_1 B - \lambda_2\left((1-u_1)\hat{\beta}(1-\eta p_2)\tfrac{S(I+A)}{N^2} + \mu\right) + \lambda_3(1-u_1)\hat{\beta}(1-\eta p_2)p_3\tfrac{S(I+A)}{N^2} \\
&\quad +\lambda_4(1-u_1)\hat{\beta}(1-\eta p_2)(1-p_3)\tfrac{S(I+A)}{N^2} - \lambda_5(-\gamma-\mu) - \lambda_6\gamma \\
\tfrac{d\lambda_6}{dt} &= -\tfrac{\partial H}{\partial R} \\
&= -\lambda_1 B - \lambda_2\left((1-u_1)\hat{\beta}(1-\eta p_2)\tfrac{S(I+A)}{N^2} + \mu\right) + \lambda_3(1-u_1)\hat{\beta}(1-\eta p_2)p_3\tfrac{S(I+A)}{N^2} \\
&\quad +\lambda_4(1-u_1)\hat{\beta}(1-\eta p_2)(1-p_3)\tfrac{S(I+A)}{N^2} + \lambda_6\mu
\end{aligned}$$

Similarly, we obtained the controls by solving the equation $\frac{\partial H}{\partial u_i} = 0$ at u_i^*, for $i = 1, 2, 3$, following Pontryagin's methods and obtained:

$$\begin{aligned}
&\tfrac{\partial H}{\partial u_1} = 0 \Leftrightarrow u_1 = \tfrac{\hat{\beta}(1-\eta p_2)[(\lambda_3-\lambda_4)p_3+\lambda_4-\lambda_2]}{w_1}\tfrac{S(I+A)}{N} \\
&\tfrac{\partial H}{\partial u_2} = 0 \Leftrightarrow u_2 = \tfrac{\lambda_3-\lambda_5}{w_2}I \\
&\tfrac{\partial H}{\partial u_3} = 0 \Leftrightarrow u_3 = \tfrac{\lambda_4-\lambda_5}{w_3}A
\end{aligned}$$

Hence,

$$\begin{aligned}
u_1^* &= \max\left\{0, \min\left\{1, \tfrac{\hat{\beta}(1-\eta p_2)[(\lambda_3-\lambda_4)p_3+\lambda_4-\lambda_2]}{w_1}\tfrac{S(I+A)}{N}\right\}\right\} \\
&= \begin{cases} 0 & \tfrac{\hat{\beta}(1-\eta p_2)[(\lambda_3-\lambda_4)p_3+\lambda_4-\lambda_2]}{w_1}\tfrac{S(I+A)}{N} \le 0, \\ \tfrac{\hat{\beta}(1-\eta p_2)[(\lambda_3-\lambda_4)p_3+\lambda_4-\lambda_2]}{w_1}\tfrac{S(I+A)}{N} & 0 < \tfrac{\hat{\beta}(1-\eta p_2)[(\lambda_3-\lambda_4)p_3+\lambda_4-\lambda_2]}{w_1}\tfrac{S(I+A)}{N} < 1, \\ 1 & \tfrac{\hat{\beta}(1-\eta p_2)[(\lambda_3-\lambda_4)p_3+\lambda_4-\lambda_2]}{w_1}\tfrac{S(I+A)}{N} \ge 1 \end{cases}
\end{aligned} \tag{9}$$

$$u_2^* = \max\left\{0, \min\left\{1, \frac{\lambda_3-\lambda_5}{w_2} I\right\}\right\} = \begin{cases} 0 & \frac{\lambda_3-\lambda_5}{w_2} I \leq 0, \\ \frac{\lambda_3-\lambda_5}{w_2} I & 0 < \frac{\lambda_3-\lambda_5}{w_2} I < 1, \\ 1 & \frac{\lambda_3-\lambda_5}{w_2} I \geq 1 \end{cases} \tag{10}$$

$$u_3^* = \max\left\{0, \min\left\{1, \frac{\lambda_4-\lambda_5}{w_3} A\right\}\right\} = \begin{cases} 0 & \frac{\lambda_4-\lambda_5}{w_3} A \leq 0, \\ \frac{\lambda_4-\lambda_5}{w_3} A & 0 < \frac{\lambda_4-\lambda_5}{w_3} A < 1, \\ 1 & \frac{\lambda_4-\lambda_5}{w_3} A \geq 1 \end{cases} \tag{11}$$

3.2. Numerical simulation

The parameter values are given in Tables 2 and 4 for simulation. Overall, the budget allocated for handling the COVID-19 pandemic reached IDR 1,895.5 trillion [31]. Details of the total annual costs of handling the COVID-19 outbreak from 2020 to 2022 were obtained from the Central Government Financial Report/Laporan Keuangan Pemerintah Pusat (LKPP) from 2020 to 2022. Some data on COVID-19 handling costs, such as vaccination and patient care costs, are not presented comprehensively and completely in the Central Government Financial Report. This information is generally obtained from statements by government officials quoted by national media, therefore, in this study it is classified as a secondary source and presented with methodological limitations. From the Central Government Financial Reports (Audited) for 2020, 2021, and 2022, information was obtained about the total annual COVID-19 handling costs, namely IDR 695.2 trillion for 2020 [36], IDR 744.77 trillion for 2021 [37], and IDR 455.6 trillion for 2022 [38]. Of this amount, expenditure for the vaccination program was recorded at IDR 57.84 trillion [32] and counseling services at IDR 0.75 trillion [33] , so that the accumulation of both is IDR 58.59 trillion. Based on this data, the weight value of $w_1 \approx 0.03$ was obtained. Meanwhile, the total cost of quarantine and treatment during the 2020–2022 period reached IDR 285.2 trillion, which came from a breakdown of IDR 62.7 trillion in 2020 [34] , and IDR 100 trillion and IDR 122.5 trillion in the following two years [35]. This results in a value of $w_2 = 0.15$. Because the cost for isolation of asymptotic infected person is less than the cost for quarantine and treated symptotic infected case person then we assumed $w_3 = 0.05$. The Confidence Interval of I and A for every control measure and given temperature can be seen at Table 5. The Confidence Intervals I and I under some particular control are given by 6 and 7 respectively.

From Table 5, the distribution of I data under single control with the lowest limit of mean (both lower and upper limits) is the distribution of I data under the control strategy u_1 and the distribution of A data under single control with the lowest limit of mean (both lower and upper limits) is the distribution of A data under the control strategy u_3. Therefore, the best single control to reduce I is the control strategy u_1 and the best single control to reduce A is the control strategy u_3. From Table 6, the distribution of I data under the influence of control u_1 at each given temperature $(7^\circ C, 10^\circ C, 22.5^\circ C, 25^\circ C)$ is the same as the distribution of I data under the influence of control $(u_1 \& u_3)$. The distribution of I data under the influence of control $(u_1 \& u_2)$ at each given temperature is the same as the distribution of I data under the influence of control $(u_1, u_2, \& u_3)$. Therefore, the implementation of the control strategy u_1 to reduce I has the same effect as the implementation of a control strategy $(u_1 \& u_3)$ and the implementation of the control strategy $(u_1 \& u_2)$ to reduce I has the same effect as the implementation of a control strategy $(u_1, u_2, \& u_3)$. The distribution of I data with the lowest limit of mean (both lower and upper limits) is the distribution of I data under the control strategy $(u_1 \& u_2)$ and control strategy $(u_1, u_2, \& u_3)$ where both strategies have the same effect. Therefore, the best strategy to reduce I is strategy $(u_1 \& u_2)$ or strategy $(u_1, u_2, \& u_3)$.

From Table 5, the distribution of A data under the influence of control u_1 at each given temperature is the same as the distribution of A data under the influence of control $(u_1 \& u_2)$. From Table 7,the distribution of A data under the influence of control $(u_1 \& u_3)$ at every given temperature is the same as the distribution of A data under the influence of control $(u_1, u_2, \& u_3)$. Therefore, the implementation of the control strategy u_1 to reduce A has the same effect as the implementation of the control strategy $(u_1 \& u_2)$ and the implementation of the control strategy $(u_1 \& u_3)$ to

Table 5. Confidence Interval of I and A

Temp ($^\circ C$)	Control Measures	Mean (I)	Std. Dev. (I)	95%CI lower (I)	95%CI upper (I)	Mean (A)	Std. Dev. (A)	95%CI lower (A)	95%CI upper (A)
7	no control	133645.71	364664.69	123537.91	143753.51	41430.64	93444.39	38840.54	44020.74
	u_1	871.02	13261.45	503.44	1238.60	3869.76	15119.27	3450.68	4288.84
	u_2	6351.98	23278.05	5706.76	6997.20	7337.00	21385.91	6744.23	7929.78
	u_3	19262.94	80057.96	17043.89	21481.99	566.11	4470.86	442.19	690.03
	$u_1\&u_2$	441.13	9670.01	173.10	709.17	3869.76	15119.27	3450.68	4288.84
	$u_1\&u_3$	871.02	13261.45	503.44	1238.60	248.35	4043.26	136.27	360.42
	$u_2\&u_3$	1039.78	14652.49	633.64	1445.92	269.80	4191.81	153.61	385.99
	$u_1, u_2, \&u_3$	441.13	9670.01	173.10	709.17	248.35	4043.26	136.27	360.42
10	no control	102373.46	270147.06	94885.51	109861.42	34656.98	76402.78	32539.24	36774.72
	u_1	812.24	12802.38	457.38	1167.09	3870.31	15121.41	3451.17	4289.44
	u_2	6213.84	22717.27	5584.16	6843.52	7382.54	21447.94	6788.05	7977.04
	u_3	12034.68	58279.52	10419.28	13650.07	456.15	4387.85	334.53	577.77
	$u_1\&u_2$	426.07	9498.83	162.78	689.36	3870.31	15121.41	3451.17	4289.44
	$u_1\&u_3$	812.24	12802.38	457.38	1167.09	248.38	4043.83	136.29	360.47
	$u_2\&u_3$	996.30	14295.49	600.06	1392.55	269.53	4192.65	153.31	385.74
	$u_1, u_2, \&u_3$	426.07	9498.83	162.78	689.36	248.38	4043.83	136.29	360.47
22.5	no control	79623.60	206370.43	73903.41	85343.79	29373.23	64034.93	27598.31	31148.16
	u_1	760.81	12386.57	417.48	1104.14	3870.85	15123.55	3451.66	4290.05
	u_2	6090.67	22203.98	5475.22	6706.12	7431.88	21516.29	6835.49	8028.27
	u_3	8372.54	46599.19	7080.90	9664.18	398.75	4350.78	278.15	519.34
	$u_1\&u_2$	411.97	9335.83	153.20	670.75	3870.85	15123.55	3451.66	4290.05
	$u_1\&u_3$	760.81	12386.57	417.48	1104.14	248.42	4044.40	136.31	360.52
	$u_2\&u_3$	956.57	13961.40	569.59	1343.55	269.29	4193.51	153.05	385.52
	$u_1, u_2, \&u_3$	411.97	9335.83	153.20	670.75	248.42	4044.40	136.31	360.52
25	no control	116810.85	312778.31	108141.24	125480.46	37850.82	84272.83	35514.93	40186.70
	u_1	840.61	13026.05	479.56	1201.67	3870.03	15120.34	3450.93	4289.14
	u_2	6280.91	22991.34	5643.64	6918.19	7359.28	21416.10	6765.67	7952.89
	u_3	14993.53	67302.06	13128.05	16859.02	501.64	4420.03	379.12	624.15
	$u_1\&u_2$	433.47	9583.36	167.84	699.11	3870.03	15120.34	3450.93	4289.14
	$u_1\&u_3$	840.61	13026.05	479.56	1201.67	248.36	4043.55	136.28	360.44
	$u_2\&u_3$	1017.54	14470.96	616.44	1418.65	269.66	4192.23	153.46	385.86
	$u_1, u_2, \&u_3$	433.47	9583.36	167.84	699.11	248.36	4043.55	136.28	360.44

Table 6. Confidence Interval of I under some specific controls

Temp ($^\circ C$)	Control Measures	Mean (I)	Std. Dev. (I)	95%CI lower (I)	95%CI upper (I)
7	u_1	871.02	13261.45	503.44	1238.60
	$u_1\&u_3$	871.02	13261.45	503.44	1238.60
	$u_1\&u_2$	441.13	9670.01	173.10	709.17
	$u_1, u_2, \&u_3$	441.13	9670.01	173.10	709.17
10	u_1	812.24	12802.38	457.38	1167.09
	$u_1\&u_3$	812.24	12802.38	457.38	1167.09
	$u_1\&u_2$	426.07	9498.83	162.78	689.36
	$u_1, u_2, \&u_3$	426.07	9498.83	162.78	689.36
22.5	u_1	760.81	12386.57	417.48	1104.14
	$u_1\&u_3$	760.81	12386.57	417.48	1104.14
	$u_1\&u_2$	411.97	9335.83	153.20	670.75
	$u_1, u_2, \&u_3$	411.97	9335.83	153.20	670.75
25	u_1	840.61	13026.05	479.56	1201.67
	$u_1\&u_3$	840.61	13026.05	479.56	1201.67
	$u_1\&u_2$	433.47	9583.36	167.84	699.11 4
	$u_1, u_2, \&u_3$	433.47	9583.36	167.84	699.11

reduce A has the same effect as the implementation of the control strategy $(u_1, u_2, \&u_3)$. The distribution of A data with the lowest limit of mean (both lower and upper limit) is the distribution of A data under the control strategy

Table 7. Confidence Interval of A under some specific controls

Temp ($^\circ C$)	Control Measures	Mean (A)	Std. Dev. (A)	95%CI lower (A)	95%CI upper (A)
7	u_3	566.11	4470.86	442.19	690.03
	$u_2\&u_3$	269.80	4191.81	153.61	385.99
	$u_1\&u_3$	248.35	4043.26	136.27	360.42
	$u_1, u_2, \&u_3$	248.35	4043.26	136.27	360.42
10	u_3	456.15	4387.85	334.53	577.77
	$u_2\&u_3$	269.53	4192.65	153.31	385.74
	$u_1\&u_3$	248.38	4043.83	136.29	360.47
	$u_1, u_2, \&u_3$	248.38	4043.83	136.29	360.47
22.5	u_3	398.75	4350.78	278.15	519.34
	$u_2\&u_3$	269.29	4193.51	153.05	385.52
	$u_1\&u_3$	248.42	4044.40	136.31	360.52
	$u_1, u_2, \&u_3$	248.42	4044.40	136.31	360.52
25	u_3	501.64	4420.03	379.12	624.15
	$u_2\&u_3$	269.66	4192.23	153.46	385.86
	$u_1\&u_3$	248.36	4043.55	136.28	360.44
	$u_1, u_2, \&u_3$	248.36	4043.55	136.28	360.44

$(u_1\&u_3)$ and control strategy $(u_1, u_2, \&u_3)$ where both strategies have the same effect. Therefore, the best strategy to reduce A is the control strategy $(u_1\&u_3)$ or the control strategy $(u_1, u_2, \&u_3)$. Therefore, based on the reduction of I and A, we can say that the best strategy to reduce both I and A is the control strategy $(u_1, u_2, \&u_3)$.

As a support for Table 5, the simulation graph of the optimal control problem related to temperature changes can be seen in Fig. 4 to Fig. 7.

From Fig. 4 to Fig. 7, in line with the results obtained from Table 5, the control strategy $(u_1, u_2, \&u_3)$ is the best strategy that can reduce the number of infected people, both symptomatic and asymptomatic, at each specific temperature. The control profiles of u_1, u_2, and u_3 for each temperature are shown in Fig. 8.

From Fig. 8(a), 8(d), 8(g), and 8(j), we see that the graphs are identical to each other. From Fig. 8(b), 8(e), 8(f), and 8(k), we see that the graphs are also identical to each other. From Fig. 8(c), 8(d), 8(g), and 8(h), we see that the graphs are also identical to each other. Therefore, the changes in regional temperature did not have much influence on the control values u_1, u_2, and u_3. Hence, we can just analyze the graphs for a single temperature. From Fig. 8(a), the graph that has the least value of u_1 for almost all time are the graph of u_1 under control strategy $(u_1, u_2, \&u_3)$. The graph of u_1 under control strategy $(u_1\&u_3)$ is almost identical to the graph of u_1 under control strategy $(u_1, u_2, \&u_3)$. From Fig. 8(b), the graph that has the least value of u_2 for almost all time are the graph of u_2 under control strategy $(u_1, u_2, \&u_3)$. The graph of u_2 under control strategy $(u_1\&u_2)$ is almost identical to the graph of u_2 under control strategy $(u_1, u_2, \&u_3)$. From Fig. 8(c), the graph that has the least value of u_3 for almost all time are the graph of u_3 under control strategy $(u_1\&u_3)$. The graph of u_3 under control strategy $(u_1, u_2, \&u_3)$ is almost identical to the graph of u_3 under control strategy $(u_1\&u_3)$.

From Fig. 8(b), 8(e), 8(f), and 8(k), it can be seen that there is some increase in the values of u_2 at some time for the control strategy $(u_1\&u_2)$ and the control strategy $(u_1, u_2, \&u_3)$. Enlarged versions of the images for both control strategies are given in Fig. 9 and Fig. 10.

From Fig. 9, the increase in u_2 starting at $t = 224.7(7^\circ C), t = 224.3(10^\circ C), t = 223.9(22.5^\circ C)$, and $t = 224.5(25^\circ C)$ is due to an increase in I at the same time. This increase in I is due to a decrease in u_1 starting at $t = 224.6(7^\circ C), t = 224.2(10^\circ C), t = 223.8(22.5^\circ C)$, and $t = 224.4(25^\circ C)$ from the maximum value of u_1 while $u_2 = 0$ and $A \neq 0$ at the same time. Due to the decrease in u_1 while at the same time $u_2 = 0$ and $A \neq 0$ resulted in the emergence of a new infection with symptoms $(I \neq 0)$.

From Fig. 10, the increase in u_2 starting at $t = 14.6(7^\circ C$ and $25^\circ C)$ and $t = 14.5(10^\circ C$ and $22.5^\circ C)$ is caused by an increase in I at the same time. This increase in I is caused by a decrease in u_1 at $t = 14.5(7^\circ C$ and $25^\circ C)$ and $t = 14.4(10^\circ C$ and $22.5^\circ C)$ from the maximum value of u_1, while there has been a decrease in u_2 starting at $t = 7.5(7^\circ C), t = 7.2(10^\circ C), t = 6.9(22.5^\circ C)$, and $t = 7.3(25^\circ C)$ and a decrease in u_3 starting at $t = 13.9$ and

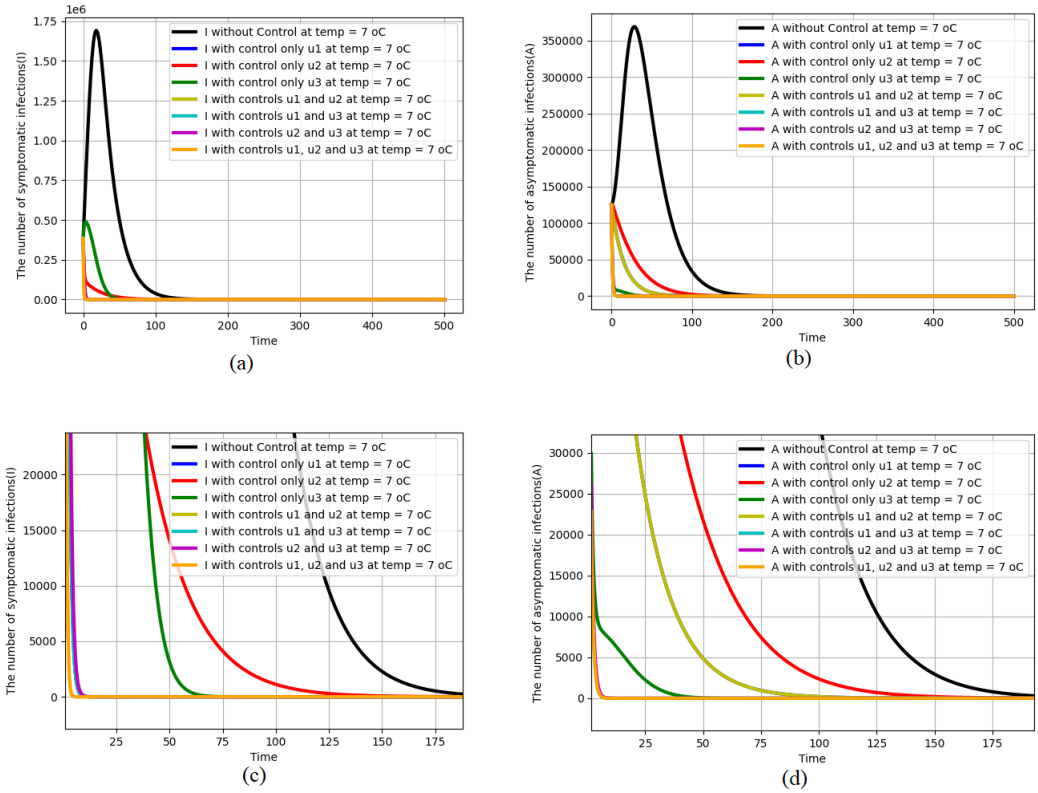

Figure 4. The graphics of (a) I, (b) A, (c) I (zoomed in mode), (d) A (zoomed in mode) at temperature $7^{\circ}C$

$A \neq 0$ at the same time. The decrease in u_1 from the maximum value of u_1 while u_2 and u_3 have also decreased at previous times, and the value of $A \neq 0$ results in the emergence of new infections with symptoms ($I \neq 0$). Therefore, a decrease in the value of u_1 when $A \neq 0$ results in the new emergence (increase) of infected people with symptoms.

3.3. Sensitivity analysis of w_1, w_2, w_3

In this section, a sensitivity analysis is performed on w_1, w_2, w_3 with a change in value of $\pm 20\%$ and the objective function using equation (6). The tornado graph is obtained as shown in Figure 11.

Based on the sensitivity analysis at various temperature variations T shown in Figure 11, a positive relationship was found between increasing control weights (w_1, w_2, w_3) and the value of the objective function J. This is in line with the principle of optimal control: a larger weight increases the cost of intervention, thereby decreasing control intensity, which in turn triggers a surge in infection rates. This effect is further amplified at high temperatures approaching the optimal transmission range. Among all variables, the control weight directly targeting infected individuals (w_2) has the most significant sensitivity level, which emphasizes the urgency of such intervention in suppressing case accum

3.4. Cost-effectiveness analysis

Economic evaluation in the context of optimal control in epidemic models is a crucial aspect in determining the most cost-efficient intervention strategy. The cost terms in the objective function represent relative penalties associated with implementing control measures, rather than empirical monetary or health-economic costs. As such, the analysis is not intended as a formal cost-effectiveness evaluation. To find the most effective and efficient way

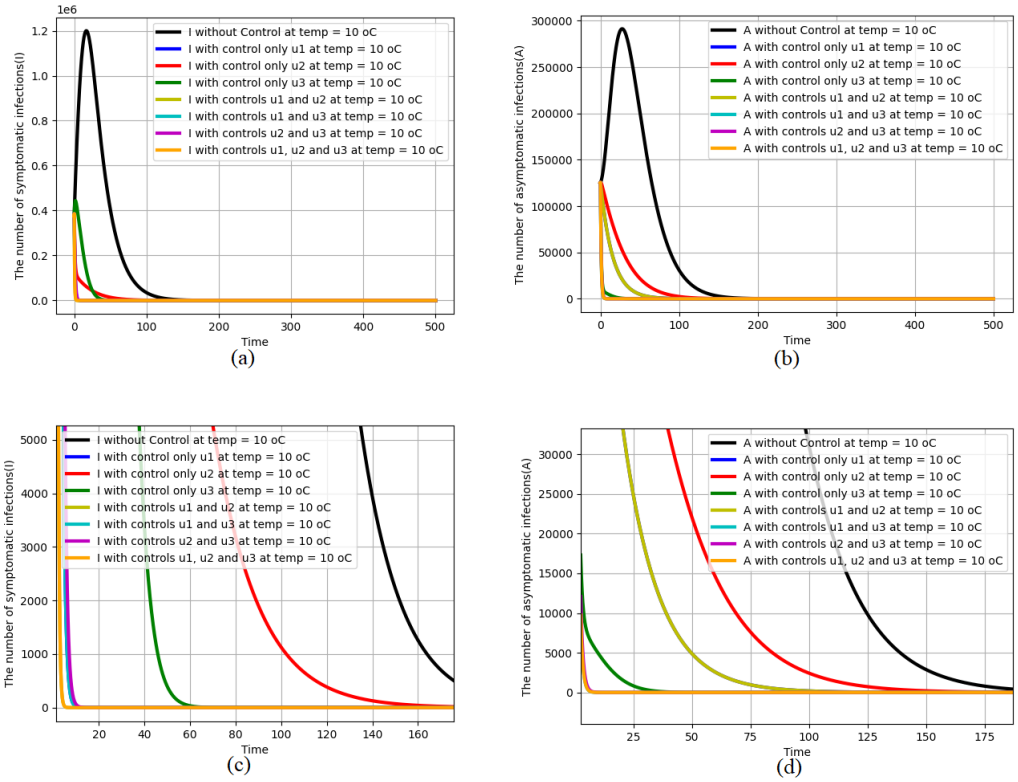

Figure 5. The graphics of (a) I, (b) A, (c) I (zoomed in mode), (d) A (zoomed in mode) at temperature $10^{\circ}C$

to control the spread of COVID-19, either with a single preventive measure or a combination of several control measures, a cost-effectiveness analysis is conducted. The goal is to ensure that the spread of the disease can be minimized with the lowest expenditure. Two key indicators commonly used in such analyses are the Average Cost-Effectiveness Ratio (ACER) and the Incremental Cost-Effectiveness Ratio (ICER) [39]. The average cost-effectiveness ratio (ACER) is calculated against a no-intervention scenario [40]. The total costs generated by the intervention are estimated using the objective function given in (6). Based on [39], the ACER is calculated as equation (12).

$$ACER = \frac{\int_0^{t_f} \left(I(t) + A(t) + \frac{1}{2}(w_1 u_1^2 + w_2 u_2^2 + w_3 u_3^2)\right)\, dx}{\text{Total number of infections averted}} \tag{12}$$

The Incremental Cost-Effectiveness Ratio (ICER) measures how much additional cost must be incurred to achieve one additional unit of health outcome. In our calculations, we assume that the total cost of implementing various control interventions will increase in proportion to the number of interventions used. The ICER formula obtained from [40] is given in equation (13)

$$ICER = \frac{\text{Difference in infection averted costs in strategies } i \text{ and } j}{\text{Difference in the total number of infections averted in strategies } i \text{ and } j} \tag{13}$$

In the ICER calculation, the numerator represents the difference between various relevant costs, including (if any) the cost of the intervention, the cost of disease prevented, and the cost of prevented productivity loss. Conversely, the denominator represents the difference in health benefits, such as the total number of infections averted, or the number of cases of susceptibility prevented from infection or carriage. The results of the ACER calculation of each strategy by using (12) are given in Table 8.

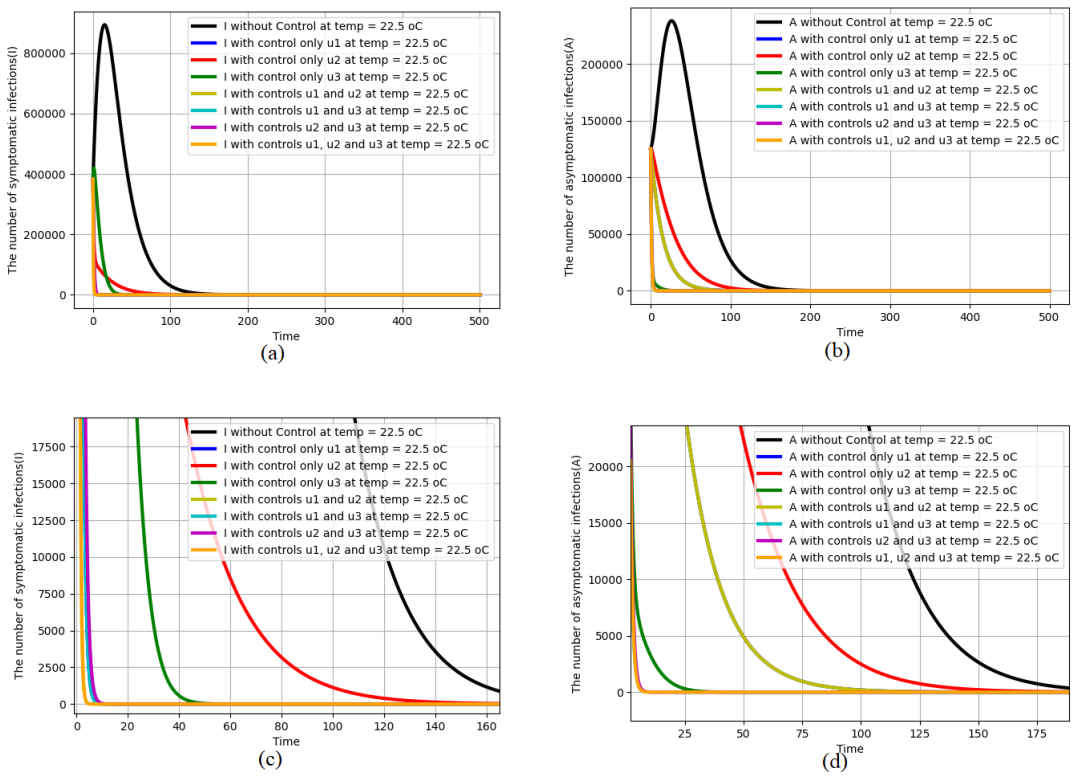

Figure 6. The graphics of (a) I, (b) A, (c) I (zoomed in mode), (d) A (zoomed in mode) at temperature $22.5°C$

The results of the ACER calculation in Table 8 show that the strategy with the lowest cost at each temperature is the control strategy $(u_1, u_2, \& u_3)$. Next, the ICER will be calculated by comparing the control scenarios sequentially, starting with the one with the fewest number of infections prevented and ending with the one with the most. The ICER calculation can be seen in Table 9.

From the ICER calculations in Table 9, it is found that single strategies (only u_1, u_2 or u_3) tend to be less efficient than combination strategies. The control strategy (u_3) at $7°C$ and $25°C$ is clearly dominated by the other strategies because it has a higher cost with a lower number of infections prevented compared to the other strategies. Likewise, the control strategy (u_2) at $10°C$ and $22.5°C$ is clearly dominated by the other strategies for the same reason. The results of sequential comparisons also show that all ICER values obtained are negative. This means that each subsequent strategy is both more effective and cheaper than the previous strategy (after being ranked based on the number of infections successfully prevented). A negative ICER value indicates strategy dominance [40], namely a strategy that is not only cheaper but also more effective than other alternatives. In this context, strategies $(u_1, u_2, \& u_3)$ are the dominant strategies.

4. Discussion

4.1. Extension to Variant-Specific Dynamics

The current model assumes fixed epidemiological parameters within each temperature scenario and does not explicitly distinguish between SARS-CoV-2 variants. This modelling choice is intended to isolate the interaction between environmental temperature and optimal control strategies under a parsimonious framework. Nevertheless,

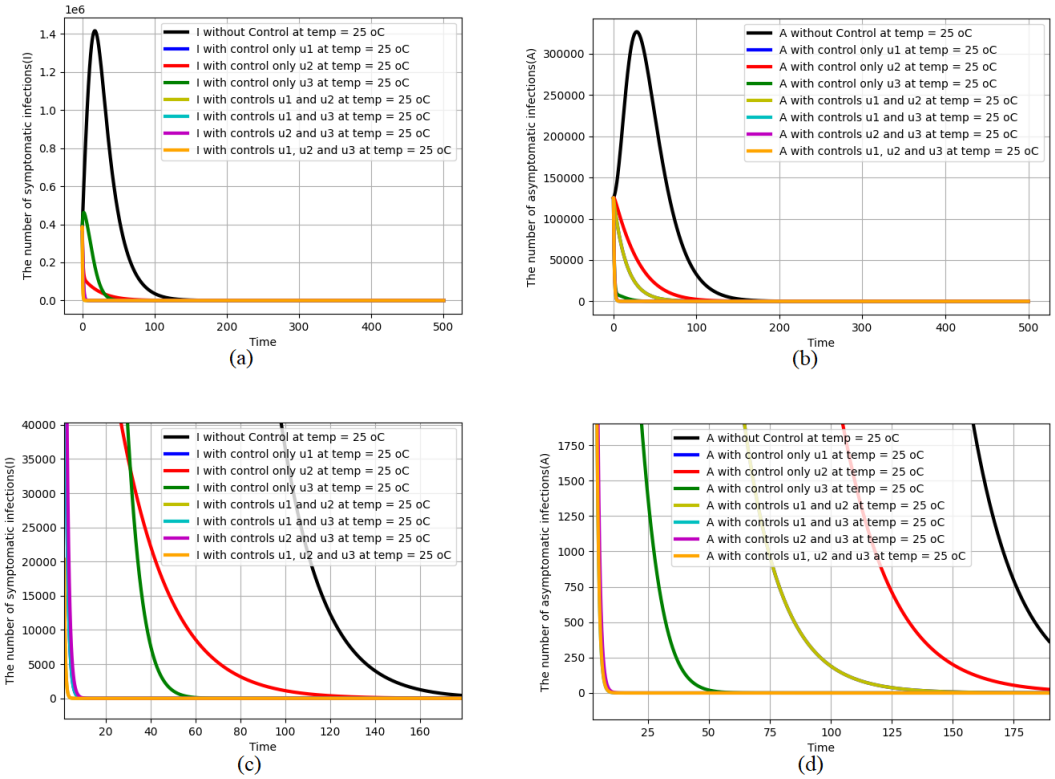

Figure 7. The graphics of (a) I, (b) A, (c) I (zoomed in mode), (d) A (zoomed in mode) at temperature $25^{\circ}C$

the proposed structure is sufficiently flexible to accommodate variant-specific characteristics observed during different pandemic waves.

In particular, variants with higher transmissibility, such as Omicron, can be incorporated by allowing the transmission rate β to become variant-dependent, for example $\beta_v(T)$, where v indexes the dominant circulating variant and T denotes temperature. Empirical evidence suggests that Omicron exhibits substantially higher transmissibility compared to earlier variants, which would correspond to an upward shift in β across temperature ranges while preserving the same fuzzy membership structure. Similarly, changes in clinical presentation associated with emerging variants can be represented through adjustments in the symptomatic proportion p_3. For variants characterized by a higher prevalence of asymptomatic or mildly symptomatic infections, p_3 can be reduced accordingly, leading to a larger asymptomatic compartment and altered control requirements. This modification does not require structural changes to the model equations, but only recalibration of parameter values within the existing framework.

From an implementation perspective, variant-specific extensions can be handled in a piecewise manner, where parameter sets $\{\beta_v, p_{3_v}\}$ are updated over time to reflect shifts in dominant variants, as identified through genomic surveillance data. Such an approach would allow the model to capture multiple epidemic waves while maintaining analytical tractability. Although variant-specific calibration is beyond the scope of the present study due to data limitations, this discussion demonstrates that the proposed fuzzy optimal control framework can readily accommodate evolving viral characteristics and remain relevant for future epidemic scenarios.

4.2. Limitations and Future Research Directions

The present study is subject to several limitations that should be acknowledged. First, there is a lack of sufficient empirical data to rigorously validate the relationship between temperature and transmission rate in the fuzzy

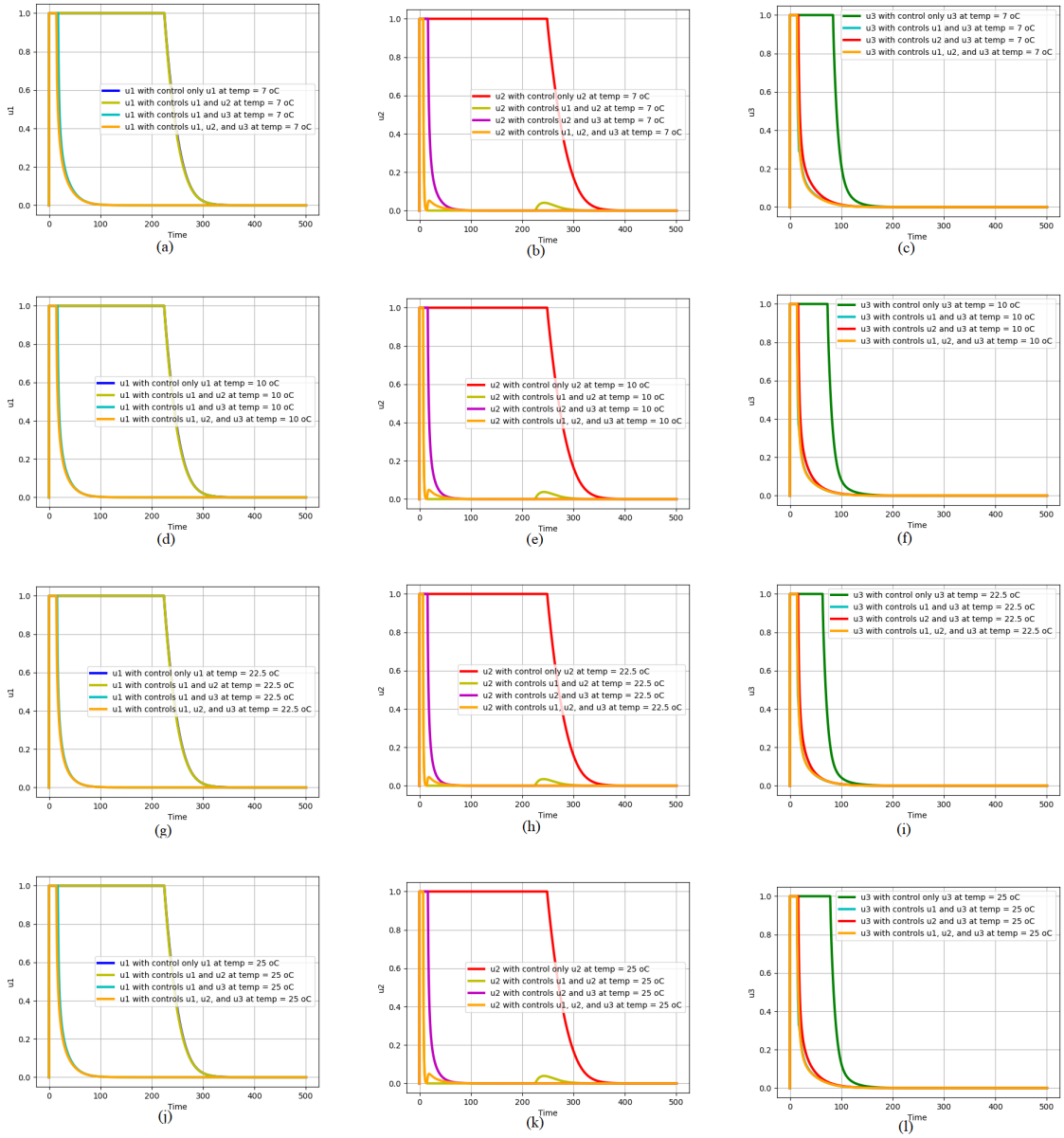

Figure 8. The graphics of profiles of (a) u_1 at $7^{\circ}C$, (b) u_2 at $7^{\circ}C$, (c) u_3 at $7^{\circ}C$, (d) u_1 at $10^{\circ}C$, (e) u_2 at $10^{\circ}C$, (f) u_3 at $10^{\circ}C$, (g) u_1 at $22.5^{\circ}C$, (h) u_2 at $22.5^{\circ}C$, (i) u_3 at $22.5^{\circ}C$, (j) u_1 at $25^{\circ}C$, (k) u_2 at $25^{\circ}C$, (l) u_3 at $25^{\circ}C$ for every control variation

parameter formulation. If the data related to the formulation of fuzzy parameters exists and is sufficient, then the fuzzy parameters can be reformulated more precisely. The assumption of constant humidity in the fuzzy parameter formulation is also another limitation. This could be a direction for further research, where fuzzy parameters are formulated using both temperature and humidity simultaneously.

Second, environmental effects are modelled using a limited number of representative temperature scenarios. This modelling choice is intended to enable qualitative comparisons of control strategies across distinct thermal regimes, rather than to identify precise temperature thresholds. Given the smooth nature of the fuzzy membership

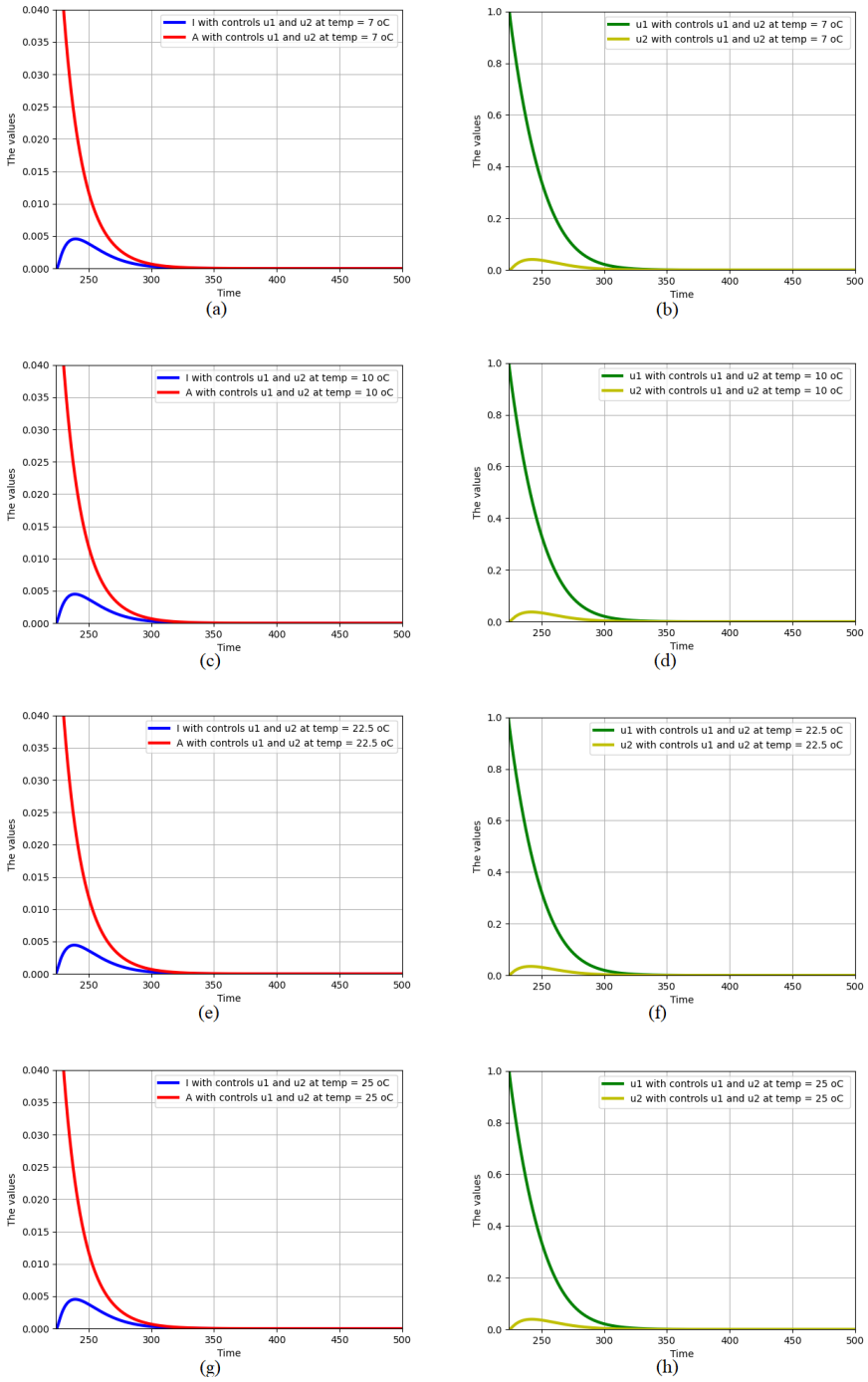

Figure 9. The graphics of (a) I, A at $7^{\circ}C$, (b) the profiles of u_1, u_2 at $7^{\circ}C$,(c) I, A at $10^{\circ}C$, (d) the profiles of u_1, u_2 at $10^{\circ}C$, (e) I, A at $22.5^{\circ}C$, (f) the profiles of u_1, u_2 at $22.5^{\circ}C$, (g) I, A at $25^{\circ}C$, (h) the profiles of u_1, u_2 at $25^{\circ}C$, for control strategy $(u_1 \& u_2)$ and $t \in [250, 500]$

functions, finer temperature increments are not expected to produce substantially different control behaviours.

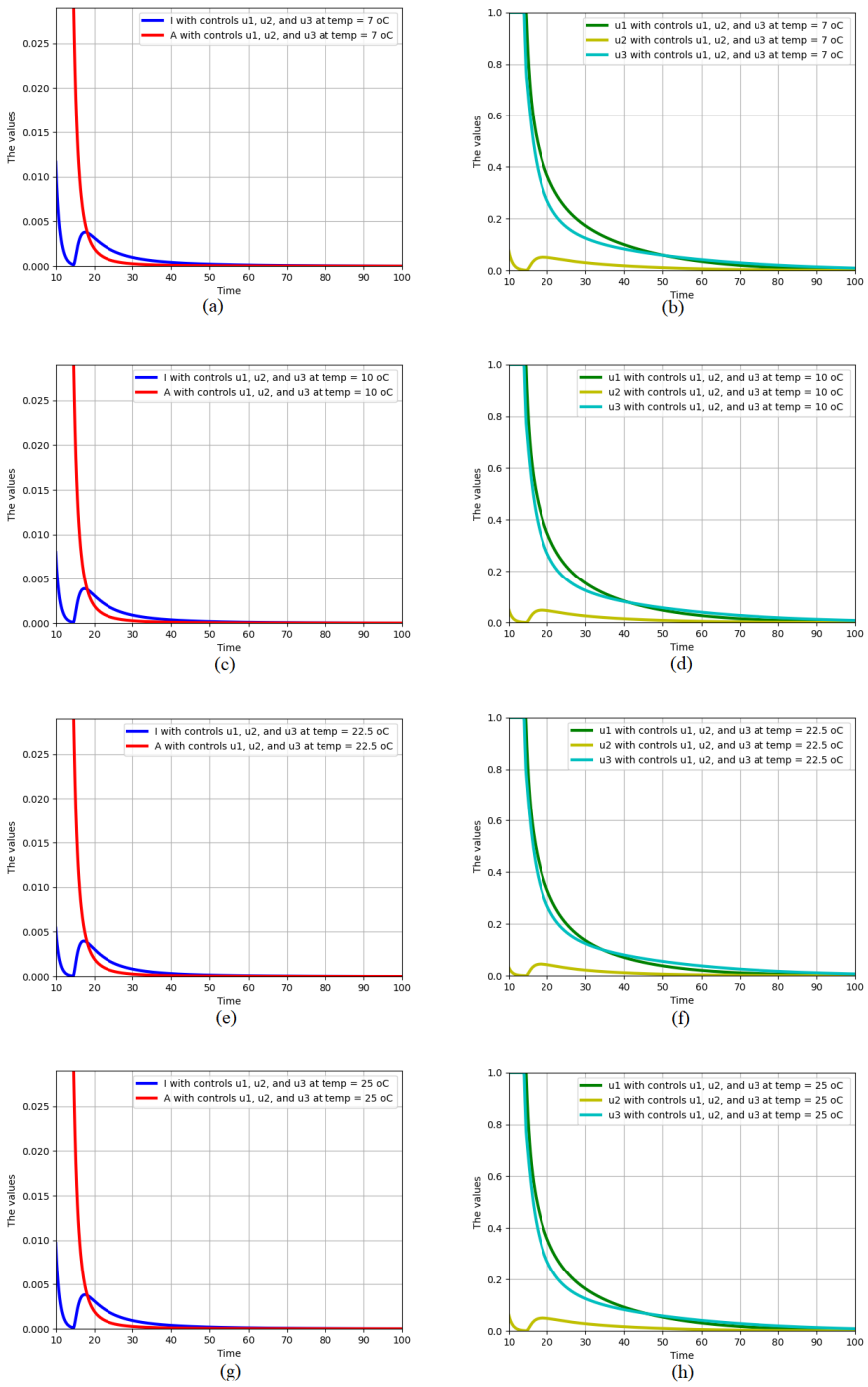

Figure 10. The graphics of (a) I, A at $7^{\circ}C$, (b) the profiles of u_1, u_2, u_3 at $7^{\circ}C$,(c) I, A at $10^{\circ}C$, (d) the profiles of u_1, u_2, u_3 at $10^{\circ}C$, (e) I, A at $22.5^{\circ}C$, (f) the profiles of u_1, u_2, u_3 at $22.5^{\circ}C$, (g) I, A at $25^{\circ}C$, (h) the profiles of u_1, u_2, u_3 at $25^{\circ}C$, for control strategy $(u_1, u_2 \& u_3)$ and $t \in [10, 100]$

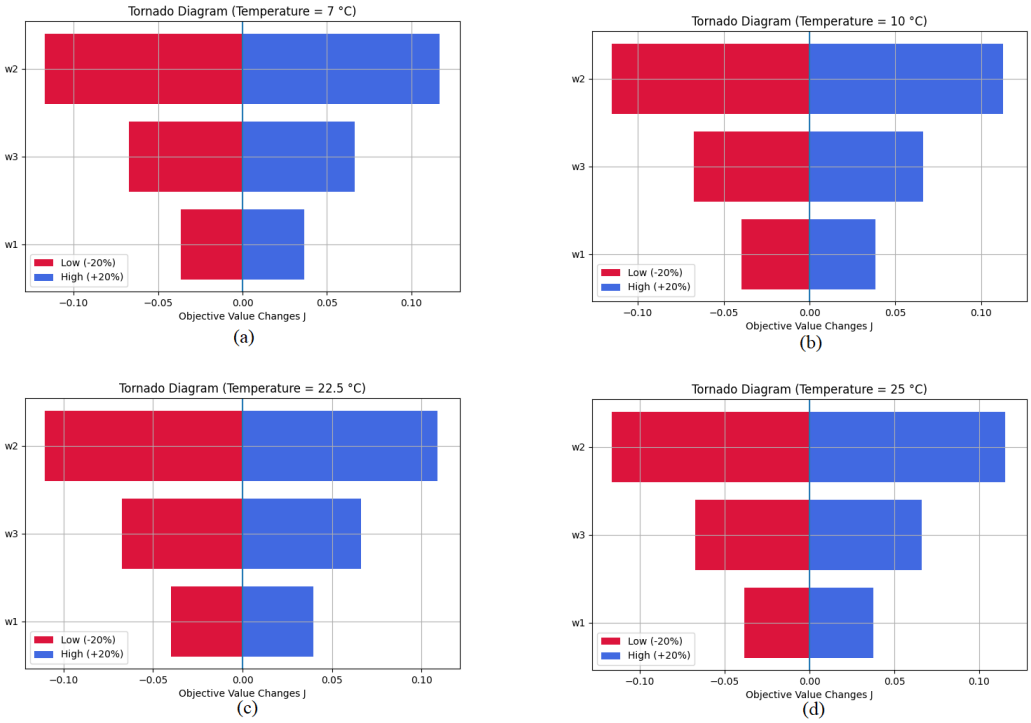

Figure 11. The Tornado diagram of objective value Changes J at (a) $7^{\circ}C$, (b) $10^{\circ}C$, (c) $22.5^{\circ}C$, (d) $25^{\circ}C$

Future studies may therefore consider employing higher-resolution temperature ranges when the identification of critical thresholds becomes a primary objective.

Third, the asymptomatic compartment $A(t)$ represents an infectious but unobserved state. Publicly available COVID-19 surveillance data in Indonesia do not provide consistent or reliable estimates of asymptomatic infectious cases, as such infections are inherently under-detected and rarely reported separately from symptomatic cases. Consequently, $A(t)$ is inferred indirectly through the model dynamics rather than calibrated against observed asymptomatic counts. Access to detailed contact tracing or workplace testing datasets would enable more rigorous estimation and validation of asymptomatic transmission in future work.

Fourth, the model assumes a homogeneous population without explicit demographic stratification by age, geography, or comorbidity status. This assumption is adopted to preserve analytical tractability and parameter identifiability within the optimal control framework, which is primarily aimed at evaluating population-level intervention trade-offs rather than subgroup-specific risks. Extending the model to stratified populations using demographic data would be a valuable direction for future research when sufficiently granular and reliable data are available.

Fifth, the control u_2 is not explicitly constrained by healthcare capacity. In practice, the implementation of this control is limited by hospital bed availability and medical infrastructure, particularly in resource-constrained regions. Future research may extend the model by introducing a hospital bed availability parameter that dynamically limits u_2, allowing the framework to better reflect regional healthcare disparities and capacity saturation effects.

Finally, there is a lack of comprehensive data in the scientific literature on the total costs of implementing control measures. Consequently, the cost weights in the objective function are treated as relative penalty parameters associated with the implementation of control measures, rather than as empirically measured economic costs. While this approach is standard in optimal control studies and facilitates transparent comparisons of intervention intensities under data limitations, future work could extend the framework by incorporating empirically derived

Table 8. ACER calculation of every strategy at different temperatures

Temp ($^\circ C$)	Control Measures	Total infections prevented	Total Costs	ACER
7	u_1	851,677,848.66	2,395,461.35	0.002812638
	u_2	806,936,827.50	6,869,579.75	0.008513157
	u_3	776,236,502.83	9,939,594.61	0.012804853
	$u_1\&u_2$	853,827,283.30	2,180,518.47	0.002553817
	$u_1\&u_3$	869,784,917.02	584,751.66	0.000672295
	$u_2\&u_3$	868,833,834.75	679,861.06	0.000782498
	$u_1, u_2, \&u_3$	871,934,351.66	369,808.74	0.000424125
10	u_1	661,739,502.47	2,366,343.04	0.003575943
	u_2	617,170,302.05	6,823,279.35	0.011055748
	u_3	622,698,081.21	6,270,483.56	0.010069862
	$u_1\&u_2$	663,670,342.92	2,173,259.55	0.003274607
	$u_1\&u_3$	679,849,135.54	555,376.86	0.000816912
	$u_2\&u_3$	678,823,066.14	657,984.93	0.000969303
	$u_1, u_2, \&u_3$	681,779,976.00	362,293.36	0.000531393
22.5	u_1	521,825,865.58	2,340,903.42	0.004485986
	u_2	477,371,466.14	6,786,359.62	0.014216098
	u_3	501,127,766.84	4,410,711.45	0.008801571
	$u_1\&u_2$	523,570,043.39	2,166,486.18	0.004137911
	$u_1\&u_3$	539,938,055.61	529,681.54	0.000981004
	$u_2\&u_3$	538,854,912.19	637,996.98	0.001183987
	$u_1, u_2, \&u_3$	541,682,233.44	355,264.29	0.000655854
25	u_1	749,755,084.67	2,380,394.70	0.003174896
	u_2	705,107,363.45	6,845,183.09	0.009708001
	u_3	695,832,468.04	7,772,654.89	0.011170296
	$u_1\&u_2$	751,790,785.10	2,176,825.22	0.002895520
	$u_1\&u_3$	767,863,436.35	569,556.67	0.000741742
	$u_2\&u_3$	766,872,306.87	668,670.77	0.000871945
	$u_1, u_2, \&u_3$	769,899,136.80	365,987.17	0.000475370

cost information from health authorities or regional health offices. Such an extension would allow the assumed cost weights to be replaced with data-informed estimates, thereby enhancing the policy relevance of the model.

5. Conclusion

From global sensitivity analysis, the parameter p_3 is the most dominant parameter in influencing system dynamics, with a very strong negative correlation with model output.Logically, if the percentage of infected people with symptoms (can be detected) increases, outbreak control is easier to implement. Conversely, if the percentage of infected people without symptoms (not yet detected) increases, outbreak control is more difficult, causing the probability of infection transmission to increase.

Sensitivity analysis of w_1, w_2, w_3 concludes that the effectiveness of epidemic control is significantly influenced by the allocation of control cost weights. Increasing the weights w_1, w_2, w_3 consistently increases the value of the objective function J, indicating that the higher the intervention costs, the lower the control intensity that can be implemented, resulting in an increased infection burden. This phenomenon reaches a tipping point at high temperatures that support optimal transmission. Specifically, control targeting infected individuals (w_2) is identified as the most sensitive factor, so prioritizing interventions in this group is key to minimizing the overall number of cases.

Using Pontryagin's maximum principle, the implementation of a strategy with full control actions $(u_1, u_2, \&u_3)$ at every temperature is significantly more effective in preventing the spread of the infection and also more cost-effective than the other strategies. Another interesting finding was the emergence of symptomatic patients again if the preventive controls (u_1) were reduced while asymptomatic patients still existed. Hence, the preventive controls

Table 9. ICER calculation at different temperatures

Temp ($^\circ C$)	Control Measures	Total infections prevented (TIP)	Total Costs (TC)	ΔTC	ΔTIP	ICER	More effective strategy
7	u_3	776,236,502.83	9,939,594.61				
	u_2	806,936,827.50	6,869,579.75	- 3,070,014.86	30,700,324.67	-0.0999	u_2
	u_1	851,677,848.66	2,395,461.35	- 4,474,118.39	44,741,021.16	-0.1000	u_1
	$u_1\&u_2$	853,827,283.30	2,180,518.47	- 214,942.88	2,149,434.64	-0.0999	$u_1\&u_2$
	$u_2\&u_3$	868,833,834.75	679,861.06	- 1,500,657.41	15,006,551.46	-0.1000	$u_2\&u_3$
	$u_1\&u_3$	869,784,917.02	584,751.66	95,109.40	951,082.26	-0.1000	$u_1\&u_3$
	$u_1, u_2, \&u_3$	871,934,351.66	369,808.74	-214,942.92	2,149,434.64	-0.0999	$u_1, u_2, \&u_3$
10	u_2	617,170,302.05	6,823,279.35				
	u_3	622,698,081.21	6,270,483.56	-552,795.79	5,527,779.16	-0.1000	u_3
	u_1	661,739,502.47	2,366,343.04	-3,904,140.53	39,041,421.26	-0.0999	u_1
	$u_1\&u_2$	663,670,342.92	2,173,259.55	-193,083.48	1,930,840.44	-0.0999	$u_1\&u_2$
	$u_2\&u_3$	678,823,066.14	657,984.93	-1,515,274.62	15,152,723.22	-0.1000	$u_2\&u_3$
	$u_1\&u_3$	679,849,135.54	555,376.86	-102,608.07	1,026,069.40	-0.1000	$u_1\&u_3$
	$u_1, u_2, \&u_3$	681,779,976.00	362,293.36	-193,083.51	1,930,840.46	-0.0999	$u_1, u_2, \&u_3$
22.5	u_2	477,371,466.14	6,786,359.62				
	u_3	501,127,766.84	4,410,711.45	-2,375,648.17	23,756,300.70	-0.1000	u_3
	u_1	521,825,865.58	2,340,903.42	-2,069,808.04	20,698,098.75	-0.0999	u_1
	$u_1\&u_2$	523,570,043.39	2,166,486.18	-174,417.24	1,744,177.81	-0.0999	$u_1\&u_2$
	$u_2\&u_3$	538,854,912.19	637,996.98	-1,528,489.19	15,284,868.80	-0.1000	$u_2\&u_3$
	$u_1\&u_3$	539,938,055.61	529,681.54	-108,315.44	1,083,143.42	-0.100	$u_1\&u_3$
	$u_1, u_2, \&u_3$	5541,682,233.44	355,264.29	-174,417.26	1,744,177.83	-0.0999	$u_1, u_2\&u_3$
25	u_3	695,832,468.04	7,772,654.89				
	u_2	705,107,363.45	6,845,183.09	-927,471.80	9,274,895.42	-0.0999	u_2
	u_1	749,755,084.67	2,380,394.70	-4,464,788.39	44,647,721.21	-0.1000	u_1
	$u_1\&u_2$	751,790,785.10	2,176,825.22	-203,569.47	2,035,700.44	-0.0999	$u_1\&u_2$
	$u_2\&u_3$	766,872,306.87	668,670.7	-1,508,154.46	15,081,521.77	-0.1000	$u_2\&u_3$
	$u_1\&u_3$	767,863,436.35	569,556.67	-99,114.10	991,129.48	-0.1000	$u_1\&u_3$
	$u_1, u_2, \&u_3$	769,899,136.80	365,987.17	-203,569.50	2,035,700.45	-0.0999	$u_1, u_2\&u_3$

(u_1) should not be reduced until it is certain that the infected person is truly free. This requires further study on how to determine whether an infected person is truly no longer present in real life.

Acknowledgement

This research was supported by the Education Fund Management Institution (LPDP) and Higher Education Financing Center (BPPT) from the Indonesian Education Scholarship Program (BPI) Ministry of Education, Culture, Research, and Technology (MoECRT).

REFERENCES

1. N. Zhu, D. Zhang, W. Wang, X. Li, B. Yang, J. Song, X. Zhao, B. Huang, W. Shi, R. Lu, P. Niu, F. Zhan, X. Ma, D. Wang, W. Xu, G. Wu, G.F. Gao, and W. Tan, *A Novel Coronavirus from Patients with Pneumonia in China, 2019*, The New England Journal of Medicine, vol. 382, no. 8, pp. 727–733, 2020. https://doi.org/10.1056/NEJMoa2001017
2. E. C. Holmes, S. A. Goldstein, A. L. Rasmussen, D. L. Robertson, A. Crits-Christoph, J. O. Wertheim, S. J. Anthony, W. S. Barclay, M. F. Boni, P. C. Doherty, J. Farrar, J. L. Geoghegan, X. Jiang, J. L. Leibowitz, S. J. D. Neil, T. Skern, S. R. Weiss, M. Worobey, K. G. Andersen, R. F. Garry, and A. Rambaut, *The origins of SARS-CoV-2: A critical review*, Cell, vol. 184, no. 19, pp. 4848–4856, 2021. https://doi.org/10.1016/j.cell.2021.08.017
3. F. Wu, S. Zhao, B. Yu, Y. -M. Chen, M. Wang, Z. -G. Song, Y. Hu, Z. -W. Tao, J. -H. Tian, Y. -Y. Pei, M. -L. Yuan, Y. -L. Zhang, F. -H. Dai, Y. Liu, Q. -M. Wang, J.-J. Zheng, L. Xu, E. C. Holmes, and Y. -Z. Zhang, *Robust uncertainty rinciples: Exact signal reconstruction from highly incomplete frequency information*, A new coronavirus associated with human respiratory disease in China. Nature, 579, pp. 265–269, 2020.

4. A. von Bogdandy, and P. Villarreal, *Critical Features of International Authority in Pandemic Response: The WHO in the COVID-19 Crisis, Human Rights and the Changing World Order (May 13, 2020)*, Max Planck Institute for Comparative Public Law & International Law (MPIL) Research Paper No. 2020-18, 2020. https://doi.org/10.2139/ssrn.3600058
5. Q. Ma, J. Liu, Q. Liu, L. Kang, R. Liu, W. Jing, Y. Wu, and M. Liu, *Global Percentage of Asymptomatic SARS-CoV-2 Infections Among the Tested Population and Individuals With Confirmed COVID-19 Diagnosis A Systematic Review and Meta-analysis* , JAMA Network Open, vol. 4, no. 12, pp. 1–18, 2021. https://doi.org/10.1001/jamanetworkopen.2021.37257
6. P. Sah, M. C. Fitzpatrick, C. F. Zimmer, E. Abdollahi, L. Juden-kelly, S. M. Moghadasc, B. H. Singer, and A. P. Galvani, *Asymptomatic SARS-CoV-2 infection: A systematic review and meta-analysis* , Proceedings of the National Academy of Sciences (PNAS), vol. 118, no. 34, pp. 1–12, 2021. https://doi.org/10.1073/pnas.2109229118
7. E. A. Triyono, J. Wahyuhadi, C. S. Waloejo, D. A. Perdana, S. D. Dewanti, A. A. Hidayat, M. A. P. Lusida, F. Sarasati, K. N. A. Dharma, M. I. Z. Al-Razzak, T. H. Wiranegara, and N. D. Ali, *Clinical Characteristics of 6102 Asymptomatic and Mild Cases for Patients with COVID-19 in Indonesia* , Pathophysiology, vol. 30, no. 3, pp. 366–376, 2023. https://doi.org/10.3390/pathophysiology30030028.
8. A. R. Anugerah, P. S. Muttaqin, and D. A. Purnama, *Effect of large-scale social restriction (PSBB) during COVID-19 on outdoor air quality: Evidence from five cities in DKI Jakarta Province, Indonesia* , Environmental Research, 197, 111164, 2021. https://doi.org/10.1016/j.envres.2021.111164
9. R. W. Tuti, A. Nurmandi, and A. Az-Zahra, *Handling COVID-19 in the capital city of Jakarta with innovation policy: the scale of social restrictions policy* , Heliyon, vol. 8, no. 5, e09467, 2022. https://doi.org/10.1016/j.heliyon.2022.e09467
10. N.R. Sasmita, M. Ikhwan, S. Suyanto, and V. Chongsuvivatwong, *Optimal control on a mathematical model to pattern the progression of coronavirus disease 2019 (COVID-19) in Indonesia* , Global Health Research and Policy, vol. 5, no. 8, 2020. https://doi.org/10.1186/s41256-020-00163-2
11. M. Kharis, Miswanto, and C. Alfiniyah, *Optimal Control Problem of Quarantined-Susceptible-Infected-Quarantined-Recovered Mathematical Model of the COVID-19 Epidemic with Fuzzy Parameter in Indonesia* , Mathematical Modelling of Engineering Problems, vol. 12, no. 5, pp. 1504–1512, 2025.
12. M. Abdy, S. Side, S. Annas, W. Nur, and W. Sanusi, *An SIR epidemic model for COVID-19 spread with fuzzy parameter: the case of Indonesia* , Advances in Difference Equations 2021:105, pp. 1–17, 2021. https://doi.org/10.1186/s13662-021-03263-6
13. KEMENKES RI, *Situasi COVID-19*, Kementerian Kesehatan Republik Indonesia, 2020.
14. Kompas. (2021, *Luhut: Angka Kematian Pasien COVID-19 yang Sudah Divaksin Sangat Rendah, 0,21%*, https://nasional.kompas.com/read/2021/07/21/20443561/luhut-angka-kematian-pasien-covid-19-yang-sudah-divaksin-sangat-rendah-021 (Date accessed: 2025-04-12).
15. Q. Bi, W. Yongsheng S. Mei, C. Ye, X. Zou, Z. Zhang, X. Liu, L. Wei, S. A. Truelove, T. Zhang, W. Gao, C. Cheng, X. Tang, X. Wu, Y. Wu, B. Sun, S. Huang, Y. Sun, J. Zhang, T. Ma, J. Lessler, and T. Feng, *Epidemiology and transmission of COVID-19 in 391 cases and 1286 of their close contacts in Shenzhen, China: a retrospective cohort study* , The Lancet Infectious Diseases, vol. 20, no. 8, 911–919, 2020. https://doi.org/10.1016/S1473-3099(20)30287-5
16. Pemerintah Pusat Indonesia, *Undang-undang (UU) Nomor 6 Tahun 2018 tentang Kekarantinaan Kesehatan* , https://peraturan.bpk.go.id/Details/90037/uu-no-6-tahun-2018 (Date accessed: 2025-04-12).
17. Pemerintah Pusat Indonesia, *Peraturan Pemerintah (PP) Nomor 21 Tahun 2020 tentang Pembatasan Sosial Berskala Besar (PSBB)*, https://peraturan.bpk.go.id/Details/135059/pp-no-21-tahun-2020 (Date accessed: 2025-04-12).
18. Satuan Tugas (Satgas) Penanganan COVID-19, *Surat Edaran (SE) Nomor 15 Tahun 2022 tentang Protokol Kesehatan Perjalanan Luar Negeri pada Masa Pandemi Corona Virus Disease 2019 (COVID-19)*, https://www.menpan.go.id/site/berita-terkini/berlaku-mulai-23-maret-inilah-aturan-satgas-covid-19-tentang-protokol-kesehatan-perjalanan-luar-negeri (Date accessed: 2025-04-12).
19. Badan Pusat Statistik, *Jumlah Penduduk menurut Wilayah dan Jenis Kelamin, INDONESIA, Tahun 2020*, https://sensus.bps.go.id/topik/tabular/sp2020/1/1/0 (Date accessed: 2023-09-02).
20. Resmawan, A. R. Nuha, and L. Yahya, *Analisis Dinamik Model Transmisi COVID-19 dengan Melibatkan Intervensi Karantina* , Jambura Journal of Mathematics, vol 3, no. 1, 66–79, 2021.
21. Hendratno, *COVID-19 Indonesia Dataset* , https://www.kaggle.com/datasets/Hendratno/covid19-indonesia (Date accessed: 2023-01-27).
22. N. M. Nasir, I. S. Joyosemito, B. Boerman, and I. Ismaniah, *Kebijakan Vaksinasi COVID-19: Pendekatan Pemodelan Matematika Dinamis Pada Efektivitas Dan Dampak Vaksin Di Indonesia* , Jurnal Pengabdian Kepada Masyarakat UBJ, vol. 4, no. 2, 191–204, 2021. https://doi.org/10.31599/jabdimas.v4i2.662
23. A. Anis, *The Effect of Temperature Upon Transmission of COVID-19: Australia And Egypt Case Study* , SSRN, 3567639, 1–20, 2020. https://dx.doi.org/10.2139/ssrn.3567639
24. A. S. Ahmar, M. A. El Safty, S. Al Zahrani, R. Rusli, and A. Rahman, *Association between temperature and relative humidity in relation to covid-19*, Intelligent Automation and Soft Computing, vol. 30, no. 3 pp. 795–803, 2021. https://doi.org/10.32604/iasc.2021.016868
25. W. Kerobe, A. S. Msellem, P. A. Sabuni, F. I. Mkassy, P. M. Chilipweli, A. Kapesa, B. R. Kidenya, P. Ayieko, D. Bintabara, and E. T. Konje, *Impact of temperature and humidity on SARS-CoV-2 transmissibility: a systematic review and meta-analysis*, Frontiers in public health, vol. 13,1570002, 2025. https://doi.org/10.3389/fpubh.2025.1570002
26. K. Y. Ng, Md. Z. Hasan, and A. Rahman, *Modelling and optimal control of pneumonia disease with cost-effective strategieExamining the roles of meteorological variables in COVID-19 spread in Malaysia*, Aerobiologia, vol. 40, pp. :129–144, 2024. https://doi.org/10.1007/s10453-023-09804-8
27. M. Liu, Z. Li, M. Liu, Y. Zhu, Y. Liu, M. William, N. Kuetche, J. Wang, X. Wang, X. Liu, X. Li, W. Wang, X. Guo, and L. Tao, *Association between temperature and COVID-19 transmission in 153 countries*, Environmental Science and Pollution Research, vol. 29, pp. 16017–16027, 2022. https://doi.org/10.1007/s11356-021-16666-5
28. G. T. Tilahun, O. D. Makinde, and D. Malonza, *Modelling and optimal control of pneumonia disease with cost-effective strategies*, Journal of Biological Dynamics, vol. 11, pp. 400—426, 2017. https://doi.org/10.1080/17513758.2017.1337245

29. M. C. Swai, N. Shaban, and T. Marijani, *Optimal Control in Two Strain Pneumonia Transmission Dynamics*, Journal of Applied Mathematics, 2021. https://doi.org/10.1155/2021/8835918
30. M. A. Rois, Trisilowati, and U. Habibah, *Optimal control of mathematical model for COVID-19 with quarantine and isolation* , International Journal of Engineering Trends and Technology, vol. 69, no. 6, pp. 154–160, 2021. https://doi.org/10.14445/22315381/IJETT-V69I6P223
31. M. Elena, *Airlangga: Total Anggaran Penanganan COVID-19 RI Rp1.895,5 Triliun*, https://ekonomi.bisnis.com/read/20220606/9/1540281/airlangga-total-anggaran-penanganan-COVID-19-ri-rp18955-triliun (Date accessed: 2025-04-12)
32. Kemenkeu, *Pemerintah Perkuat Program Penanganan Kesehatan untuk Merespon Peningkatan Kasus COVID-19*, https://menpan.go.id/site/berita-terkini/pemerintah-perkuat-program-penanganan-kesehatan-untuk-merespon-peningkatan-kasus-covid-19 (Date accessed: 2025-04-12)
33. TEMPO.CO, *Sri Mulyani Rinci Tambahan Anggaran Kesehatan Pandemi COVID-19 Rp 214 Triliun*, https://www.tempo.co/ekonomi/sri-mulyani-rinci-tambahan-anggaran-kesehatan-pandemi-COVID-19-rp-214-triliun-493412 (Date accessed: 2025-04-12)
34. FIN.CO.ID, *Biaya Pengobatan dan Perawatan Pasien COVID-19 di 2020 Capai Rp62,7 Triliun*, https://fin.co.id/2021/09/08/biaya-pengobatan-dan-perawatan-pasien-COVID-19-di-2020-capai-rp627-triliun (Date accessed: 2025-04-12)
35. A.A. Said, *Biaya Perawatan Pasien COVID-19 Tembus Rp 100 T pada 2021*, https://katadata.co.id/finansial/makro/622f170fb6c89/biaya-perawatan-pasien-COVID-19-tembus-rp-100-t-pada-2021 (Date accessed: 2025-04-12)
36. Pemerintah Republik Indonesia, *Laporan Keuangan Pemerintah Pusat Tahun 2020 (Audited) pp. 44*, https://media.kemenkeu.go.id/getmedia/3421d280-da5a-4e63-8bab-d38c8633bacc/lkpp-2020.pdf (Date accessed: 2026-01-14)
37. Pemerintah Republik Indonesia, *Laporan Keuangan Pemerintah Pusat Tahun 2021 (Audited) pp. 141*, https://media.kemenkeu.go.id/getmedia/104fbe41-1b5d-4d09-a79e-7df823863f75/LKPP-2021.pdf (Date accessed: 2026-01-14)
38. Pemerintah Republik Indonesia, *Laporan Keuangan Pemerintah Pusat Tahun 2022 (Audited) pp. 41*, https://media.kemenkeu.go.id/getmedia/dca93798-033d-4d61-9a4f-bf112fd834ab/LKPP_2022.pdf (Date accessed: 2026-01-14)
39. M. A. Rois, Fatmawati, C. Alfiniyah, S. Martini, D. Aldila, and F. Nyabadza, *Modeling and optimal control of COVID-19 with comorbidity and three-dose vaccination in Indonesia* , Journal of Biosafety and Biosecurity, vol. 6, no. 3, pp. 181–195, 2024. https://doi.org/https://doi.org/10.1016/j.jobb.2024.06.004
40. F. B. Agusto, and M. C. A. Leite, *Optimal control and cost-effective analysis of the 2017 meningitis outbreak in Nigeria* , Infectious Disease Modellin, vol. 4, no. 2, pp. 161–187, 2019. https://doi.org/10.1016/j.idm.2019.05.003